Applied Mathematics and Computation 260 (2015) 292–313

Contents lists available at ScienceDirect

Applied Mathematics and Computation

journal homepage: www.elsevier.com/locate/amc

Diffusion driven instability and Hopf bifurcation in spatial predator-prey model on a circular domain

Walid Abid [a], Radouane Yafia [b,*], M.A. Aziz-Alaoui [c], Habib Bouhafa [a], Azgal Abichou [a]

[a] University of Tunis El Manar, National Engineering School of Tunis, Laboratory of Engineering Mathematics EPT, Box: 743, La Marsa 2078, Tunisia
[b] Université Ibn Zohr, Faculté Polydisciplinaire de Ouarzazate, B.P:638, Ouarzazate, Morocco
[c] Normandie Univ, France; ULH, LMAH, F-76600 Le Havre; FR CNRS 3335, 25 rue Philippe Lebon 76600 Le Havre, France

ARTICLE INFO

Keywords:
Predator-prey model
Local and global stability
Hopf and Turing bifurcation
Pattern formation
Chaos
Disc domain

ABSTRACT

In this paper, we investigate theoretically and numerically a 2-D spatio-temporal dynamics of a predator-prey mathematical model which incorporates the Holling type *II* and a modified Leslie–Gower functional response and logistic growth of the prey. This system is modeled by a reaction diffusion equations defined on a disc domain $\{(x, y) \in \mathbb{R}^2 / x^2 + y^2 < R^2\}$ with Dirichlet initial conditions and Neumann boundary conditions. We study the local and global stability of the positive equilibrium point. We show that the diffusion can induce instability of the uniform equilibrium point which is stable with respect to a constant perturbation as shown by Turing in 1950s and derive the conditions for Hopf and Turing bifurcation in the spatial domain. Numerical results are given in order to illustrate how biological processes affect spatiotemporal pattern formation in a spatial domain. We perform the computations and generalize, on a circular domain, the results presented in Camara and Aziz-Alaoui [6].

1. Introduction and mathematical model

Most natural phenomena are modeled by a reaction diffusion systems which are special cases of systems of parabolic partial differential equations [13]. These systems of reaction–diffusion equations describe how the concentration or density distributed in space varies under the influence of two processes: local interactions of species, and diffusion that causes the spread of species in the space. These systems of equations can describe the dynamic processes in biology, physics and ecology. Predator prey dynamics are a classic and relatively well-studied example of interactions. The simplest reaction–diffusion models for cyclic populations involve two interacting species, with densities u and v:

$$\begin{cases} \dfrac{\partial}{\partial t}u(t,x) = D_u \dfrac{\partial^2}{\partial x^2}u(t,x) + f(u(t,x), v(t,x)) \\ \dfrac{\partial}{dt}v(t,x) = D_v \dfrac{\partial^2}{\partial x^2}v(t,x) + g(u(t,x), v(t,x)) \end{cases} \tag{1.1}$$

* Corresponding author. Tel.: +212666172458.
E-mail addresses: abidwalid007@yahoo.fr (W. Abid), yafia1@yahoo.fr, yafia_radouane@hotmail.com (R. Yafia), aziz.alaoui@univ-lehavre.fr (M.A. Aziz-Alaoui), HabibBouhafa@yahoo.fr (H. Bouhafa), azgal.abichou@ept.rnu.tn (A. Abichou).

http://dx.doi.org/10.1016/j.amc.2015.03.070
0096-3003/

where $f(u, v)$ and $g(u, v)$ model the local activity (absence of diffusion), the densities u and v may represent the predator and prey, host and parasite, herbivore and grazer, etc. Here x is the spatial coordinate and t denotes the time. Our focus on cyclic populations means that we assume that the local dynamics f and g are such that the spatially uniform equations $\frac{du}{dt} = f(u, v)$; $\frac{dv}{dt} = g(u, v)$ have a stable periodic solution (limit cycle), which oscillates around the unstable coexistence steady state.

The model under consideration is a 2-D reaction diffusion model which based on the predator prey system and integrates the Holling-type-*II* and a modified Leslie–Gower functional responses.

$$\begin{cases} \dfrac{\partial U(T,x,y)}{\partial T} = D_1 \Delta U(T,x,y) + \left(a_1 - b_1 U(T,x,y) - \dfrac{r_1 V(T,x,y)}{U(T,x,y)+K_1}\right) U(T,x,y), \\ \dfrac{\partial V(T,x,y)}{\partial T} = D_2 \Delta V(T,x,y) + \left(a_2 - \dfrac{r_2 V(T,x,y)}{U(T,x,y)+K_2}\right) V(T,x,y). \end{cases} \tag{1.2}$$

This two species food chain model describes a prey population U which serves as food for a predator V. $U(T, x, y)$ and $V(T, x, y)$ represent population densities at time T and space (x, y) defined on a disc domain with radius R (i.e. $\Omega = \{(x, y) \in \mathbb{R}^2 / x^2 + y^2 < R^2\}$). $\Delta = \frac{\partial^2}{\partial x^2} + \frac{\partial^2}{\partial y^2}$ is the Laplacian operator. The model parameters $r_1, a_1, b_1, k_1, r_2, a_2$ and k_2 are assuming positive values. These parameters are defined as follows: a_1 is the growth rate of preys U, a_2 describes the growth rate of predators V, b_1 measures the strength of competition among individuals of species U, r_1 is the maximum value of the per capita reduction of U due to V, r_2 has a similar meaning to r_1, k_1 measures the extent to which environment provides protection to prey U, k_2 has a similar meaning to k_1 relatively to the predator V and D_1, D_2 are the diffusion coefficients of the preys and the predators.

In this model (1.2) the first equation $(1.2)_1$ is standard. By contrast, the second equation $(1.2)_2$ is absolutely not standard. It contains a modified Leslie–Gower term, that is the second term on the right-hand side in the second equation of $(1.2)_2$; the last depicts the loss in the predator population.

The Leslie–Gower type model is given by the assumption that the reduction in predator population has a reciprocal relationship with per capita availability of its preferred food, the carrying capacity of the predator V environment is proportional to the number of prey U, that is, it depends on the available resources. He stresses the fact that there are upper limits to the rates of increase of both prey U and predator V, which are not recognized in the Lotka Volterra model. In the case of continuous time, it is $\frac{\partial V}{\partial T} = a_2 V(1 - \frac{V}{\omega U})$, in which the growth of predator population takes logistic form ($\frac{\partial V}{\partial T} = a_2 V(1 - \frac{V}{K})$).

It is assumed that $K_V = K(U) = \omega U$, i.e., the carrying capacity is proportional to the prey abundance, just as it is assumed in May–Holling–Tanner model (ω is the conversion factor of prey into predators). The term $\frac{V}{\omega U}$ is called the Leslie–Gower term. We will suppose that the predators have an alternative food when the quantity of prey U decreases, that is $K(U) = \omega U + \alpha$ (modified Leslie–Gower model). In the absence of prey U i.e. $U = 0$, then $K(U) = \alpha$ and the predator V becomes generalist since it has an alternative food. The equation above is written as $\frac{\partial V}{\partial T} = a_2 V(1 - \frac{V}{\omega U + \alpha})$, therefore $\frac{\partial V}{\partial T} = V(a_2 - (\frac{a_2}{\omega})(\frac{V}{(U + \frac{\alpha}{\omega})}))$ which is the second equation of system (1.2).

The first model proposed in this optic is given by an ordinary differential equations (see [2]) and reads as follows:

$$\begin{cases} \dfrac{dx}{dt} = \left(a_1 - b_1 x - \dfrac{r_1 y}{x + k_1}\right) x, \\ \dfrac{dy}{dt} = \left(a_2 - \dfrac{r_2 y}{x + k_2}\right) y, \end{cases} \tag{1.3}$$

with initial conditions $x(0) > 0$ and $y(0) > 0$. This two species food chain model describes a prey population x which serves as food for a predator y.

A delayed version of (1.3) (see [5]) is given by a system of two delayed differential equations as follows:

$$\begin{cases} \dfrac{dx(t)}{dt} = \left(a_1 - b_1 x(t) - \dfrac{r_1 y(t)}{x(t) + k_1}\right) x(t), \\ \dfrac{dy(t)}{dt} = \left(a_2 - \dfrac{r_2 y(t - \tau)}{x(t - \tau) + k_2}\right) y(t). \end{cases} \tag{1.4}$$

Here, the discrete delay $\tau > 0$ has been incorporated in the negative feedback of the predator's density. The notion of global stability is studied by many authors in the predator-prey systems with delay [3,15]. In [2], authors studied the boundedness and global stability of system (1.3) and in [5] authors studied the global stability and persistence of the delayed system (1.4) by using Lyapunov functional.

The existence of periodic solutions and their stability of Eq. (1.2) are studied in [22,23], by considering the time delay as a parameter of bifurcation.

The spatio-temporal predator prey model without modification is given as follows (see Huang et al. [18])

$$\begin{cases} \dfrac{\partial}{dt} u(t,x) = d_1 \dfrac{\partial^2}{\partial x^2} u(t,x) + u(t,x)\left(a_1 - \dfrac{1}{K} u(t,x) - B\dfrac{v(t,x)}{Eu(t,x)+1}\right), \\ \dfrac{\partial}{dt} v(t,x) = d_2 \dfrac{\partial^2}{\partial x^2} v(t,x) + v(t,x)\left(a_2 - Cv(t,x) + D\dfrac{u(t,x)}{Eu(t,x)+1}\right), \end{cases} \tag{1.5}$$

where all parameters in (1.5) are positives. For the meaning of all constants in (1.5) (see [18]), in which authors studied the existence of traveling waves by using shooting argument method. The corresponding model in 1-D is given by:

$$\begin{cases} \dfrac{\partial}{dt}u(t,x) = d_1\dfrac{\partial^2}{\partial x^2}u(t,x) + u(t,x)\left(a_1 - b_1u(t,x) - \dfrac{r_1v(t,x)}{u(t,x)+k_1}\right), \\ \dfrac{\partial}{dt}v(t,x) = d_2\dfrac{\partial^2}{\partial x^2}v(t,x) + v(t,x)\left(a_2 - \dfrac{r_2v(t,x)}{u(t,x)+k_2}\right), \end{cases} \tag{1.6}$$

This system is studied by Camara et al. [4,6], they show the dynamics and the asymptotic behavior of the system and prove the occurrence of Turing and Hopf patterns formation, see also [20,21]. In [24], the authors show the existence of periodic traveling waves via Hopf bifurcation theorem by considering the diffusion as a parameter of bifurcation.

Therefore, in the recent decades, a number of works have been devoted to the studies of the dynamic relationship between predators and their prey. The local dynamics has been studied in [2,4–6,10] of two dimensional and the global dynamics has been studied in [14]. Similar three dimensional systems with the same functional responses are studied in [1,8,11,12,16]. In [26,27], the authors showed the conditions of Turing instability, the role of diffusion coefficients in Turing instability and the spatiotemporal distributions of interacting species through Turing instability in two dimensional spatial domain of the predator-prey model with ratio-dependent functional response and with sigmoid (Holling type *III*) ratio-dependent functional response respectively.

Our goal, in this paper, is to generalize the results presented in 1-D (see [6]) to 2-D reaction diffusion system defined on a circular domain. We prove the local and global stability of the positive steady state and show how diffusion destabilizes stable equilibrium and is responsible for the initiation of spatial patterns. Our theoretical results are illustrated by numerical simulations.

This work is organized as follows: In Section 2, we recall some results on the model without diffusion with some results on eigenvalue problem of the Laplacian operator defined on a circular model. In Section 3, we prove the existence of the equilibrium points and the local stability of the nontrivial steady state and the boundedness of solutions. Section 4 is devoted to the global stability of the nontrivial steady state. The Turing instability is showed in Section 5. In Section 6, we illustrate our results by numerical simulations. In the end, we give a conclusion.

2. Preliminaries

2.1. Asymptotic behavior of ODE system

In this subsection we recall some results on the asymptotic behavior of the system without diffusion (1.3).

To simplify system (1.3) we introduce some transformations of variables. After applying the following rescaling

$$t = a_1T, \quad u(t) = \frac{b_1}{a_1}x(T), \quad v(t) = \frac{r_2b_1}{a_1a_2}y(T), \quad a = \frac{a_2r_1}{a_1r_2}, \quad b = \frac{a_2}{a_1}, \quad e_1 = \frac{b_1k_1}{a_1}, \quad e_2 = \frac{b_1k_2}{a_1}, \tag{2.1}$$

system (1.3) becomes

$$\begin{cases} \dfrac{du}{dt} = \left(1 - u - \dfrac{av}{u+e_1}\right)u, \\ \dfrac{dv}{dt} = \left(b - \dfrac{bv}{u+e_2}\right)v, \end{cases} \tag{2.2}$$

We also require that $ae_2 < e_1$ which ensures that, system (1.6) has a positive equilibrium point corresponding to constant coexistence of the two species. System (2.2) has forth equilibrium points: $E_0 = (0,0)$, $E_1 = (1,0)$, $E_2 = (0,e_2)$, $E^* = (u^*, v^*)$ which are equilibria of the corresponding ordinary differential equation system (2.2) without diffusion, where

$$u^* = \frac{1 - a - e_1 + \sqrt{(a+e_1-1)^2 + 4(e_1 - ae_2)}}{2}, \tag{2.3}$$

and

$$v^* = u^* + e_2. \tag{2.4}$$

Without diffusion, the equilibrium point E_0 corresponding to the absence of both species is unstable, E_1 corresponding to the prey at the environment carrying capacity in the absence of predators is a saddle point. If $ae_2 < e_1$, E_2 corresponding to the predator at the environment carrying capacity in the absence of prey is also a saddle point and E^* corresponding to coexistence of the two species is asymptotically stable if $p(u^*) > 0$ and unstable if $p(u^*) < 0$, where

$$p(x) = 2x^2 + (b + e_1 - 1)x + be_1. \tag{2.5}$$

Furthermore, E^* is asymptotically stable if $b + e_1 - 1 \geq 0$ or $0 < u^* < \alpha_1$ or $\alpha_2 < u^* < 1$ and it is unstable if $b + e_1 - 1 > 0$ and $\alpha_1 < u^* < \alpha_2$, where α_1 and α_2 are the roots of the polynomial $p(x)$:

$$\alpha_{1,2} = \frac{1 - b - e_1 \pm \sqrt{(b+e_1-1)^2 + 8be_1}}{4}.$$

Particulary, if $e_1 - 1 \geq 0$, E^* is globally asymptotically stable. If $b + e_1 - 1 \geq 0$ the system has no limit cycle.

2.2. Eigenvalue problem on a circular domain

In this subsection we give some results on the Laplace operator on a circular domain, because there exist a difference between the analysis in a rectangle domain and in a circular domain (disc).

Let us consider a disc with a radius R as follows:

$$\mathcal{D} = \{(r,\theta) : 0 \le r < R,\ 0 \le \theta < 2\pi\}.$$

Then, the Laplace operator is defined in cartesian coordinates as $\Delta\varphi = \frac{\partial^2}{\partial x^2}\varphi + \frac{\partial^2}{\partial y^2}\varphi$ and in polar coordinates (r,θ) as $\Delta_{r\theta}\varphi = \frac{\partial^2}{\partial r^2}\varphi + \frac{1}{r}\frac{\partial}{\partial r}\varphi + \frac{1}{r^2}\frac{\partial^2}{\partial \theta^2}\varphi$, with $x = r\cos(\theta)$ and $y = r\sin(\theta)$ and $r = \sqrt{x^2+y^2}$ and $\tan(\theta) = \frac{y}{x}$.

To compute the eigenvectors on the circular domain, one need to separate variables using polar coordinates. Considering the following eigenvalue problem:

$$\begin{cases} \Delta_{r\theta}\varphi = -\lambda\varphi, \\ \varphi(R,\theta) = 0,\ \theta \in [0, 2\pi], \\ \frac{\partial\varphi}{\partial r} = 0,\ \text{on } r = R \text{ and } \theta \in [0, 2\pi] \end{cases} \tag{2.6}$$

and looking for solutions of the form $\varphi(r,\theta) = P(r)\Phi(\theta)$. By differentiation and from the Eq. (2.6) we have:

$$\begin{cases} P''(r)\Phi(\theta) + \frac{1}{r}P'(r)\Phi(\theta) + \frac{1}{r^2}P(r)\Phi''(\theta) = -\lambda P(r)\Phi(\theta), \\ P(R) = P'(R) = 0. \end{cases} \tag{2.7}$$

Therefore

$$\frac{r^2}{P(r)}\left\{P''(r) + \frac{1}{r}P'(r) + \lambda P(r)\right\} = -\frac{\Phi''(\theta)}{\Phi(\theta)}. \tag{2.8}$$

Since the function $\Phi(\theta)$ is 2π-periodic, there exists k such that $-\Phi''(\theta) = k^2\Phi(\theta)$ and $\Phi(0) = \Phi(2\pi)$, $\Phi'(0) = \Phi'(2\pi)$. The solution is given by:

$$\Phi_n(\theta) = a_n\sin(n\theta) + b_n\cos(n\theta) \text{ for integers } k = n \ge 0$$

where a_n and b_n are constants.

Then we have the following second order differential equation

$$P''(r) + \frac{1}{r}P'(r) + \left(\lambda - \frac{k^2}{r^2}\right)P(r) = 0,\ \text{such that } P'(R) = 0,\ P(R) = 0. \tag{2.9}$$

Let $x = \sqrt{\lambda}r$ and $P(r) = P(\frac{x}{\sqrt{\lambda}}) = J(x)$. Then, we have

$$J''(x) + \frac{1}{x}J'(x) + \left(1 - \frac{k^2}{x^2}\right)J(x) = 0 \text{ (called Bessel equation)}. \tag{2.10}$$

The solution for it is the nth Bessel function

$$J_n(x) = \sum_{l=0}^{+\infty}\frac{(-1)^l}{l!\,(n+l)!}\left(\frac{x}{2}\right)^{n+2l}.$$

Since $P(r) = J_n(\sqrt{\lambda}r)$, we get:

$$\phi_n^\lambda(r,\theta) = \Phi_n(\theta)J_n(\sqrt{\lambda}r) \tag{2.11}$$

are eigenfunctions of the Laplacian operator in polar coordinates.

The eigenvalues λ associated to the eigenvector ϕ_n^λ are determined from the boundary conditions.

From Dirichlet boundary conditions defined as follows $\phi_n^\lambda(R,\theta) = 0, \forall\theta \in [0, 2\pi]$ which imply that: $J_n(\sqrt{\lambda}R) = 0$. This means that $\sqrt{\lambda}R$ is a root of J_n.

From the Neumann boundary conditions: $\partial_r\phi_n^\lambda(R,\theta) = 0, \forall\theta \in [0, 2\pi]$ which imply that: $J_n'(\sqrt{\lambda}R) = 0$. This means that $\sqrt{\lambda}R$ is a root of J_n'.

We note these roots by α_{nm} and we assume they are indexed in increasing order:

$$J_n(\alpha_{nm}) = 0, \alpha_{n1} < \alpha_{n2} < \alpha_{n3} < \cdots$$

Therefore $\sqrt{\lambda}R = \alpha_{nm}$ for some index m and the eigenvalues will be written in the following form:

$$\lambda_{nm} = \left(\frac{\alpha_{nm}}{R}\right)^2$$

where n is the index of Bessel function and m is the index number of their roots.

If $R = 1$, then the eigenvalues of the equations $\Delta\varphi = -\lambda\varphi$ are the square of zero solution of Bessel functions (see Fig. 1).

3. Equilibrium points and stability

Let us now consider the reaction diffusion system defined on a circular domain with Neumann boundary conditions (which means there are no flux of species of both the predator and prey on the boundary of the circular domain) and Dirichlet initial conditions as follow:

$$\begin{cases} \dfrac{\partial U(T,x,y)}{\partial T} = \delta_1 \Delta U(T,x,y) + (a_1 - b_1 U(T,x,y) - \dfrac{c_1 V(T,x,y)}{U(T,x,y)+K_1})U(T,x,y), \text{ for } T \in [0,+\infty[, (x,y) \in \Omega, \\ \dfrac{\partial V(T,x,y)}{\partial T} = \delta_2 \Delta V(T,x,y) + (a_1 - \dfrac{c_2 V(T,x,y)}{U(T,x,y)+K_2})V(T,x,y), \text{ for } T \in [0,+\infty[, (x,y) \in \Omega, \\ \nabla U(\cdot,x,y)\cdot\eta = \nabla V(\cdot,x,y)\cdot\eta = 0; \text{ on } \partial\Omega \text{ Neumann boundary conditions}, \\ U(0,\cdot,\cdot) = U_0(\cdot,\cdot) \text{ and } V(0,\cdot,\cdot) = V_0(\cdot,\cdot); \text{ Dirichlet initial conditions}, \end{cases} \tag{3.1}$$

where $\Omega = \{(x,y) \in \mathbb{R}^2 / x^2 + y^2 < R^2\}$.

By the following dimensionless:

$$t = a_1 T, \quad u(t) = \frac{b_1}{a_1} U(T), \quad v(t) = \frac{c_2 b_1}{a_1 a_2} V(T), \quad r' = r\left(\frac{a_1}{\delta_1}\right)^{\frac{1}{2}}, \quad \theta' = \theta\left(\frac{a_1}{\delta_1}\right)^{\frac{1}{2}}, \tag{3.2}$$

$$a = \frac{a_2 c_1}{a_1 c_2}, \quad b = \frac{a_2}{a_1}, \quad e_1 = \frac{b_1 k_1}{a_1}, \quad e_2 = \frac{b_1 k_2}{a_1}, \quad \delta = \frac{\delta_2}{\delta_1}, \tag{3.3}$$

system (3.1) reads as:

$$\begin{cases} \dfrac{\partial u(t,x,y)}{\partial t} = \Delta u(t,x,y) + u(t,x,y)(1-u(t,x,y)) - \dfrac{a v(t,x,y)}{u(t,x,y)+e_1} u(t,x,y); \text{ for } t \in [0,+\infty[, (x,y) \in \Omega, \\ \dfrac{\partial v(t,x,y)}{\partial t} = \delta \Delta v(t,x,y) + b(1 - \dfrac{v(t,x,y)}{u(t,x,y)+e_2})v(t,x,y), \text{ for } t \in [0,+\infty[, (x,y) \in \Omega, \\ \nabla u(\cdot,x,y).\eta = \nabla v(\cdot,x,y).\eta = 0 \text{ on } \partial\Omega; \text{ Neumann boundary conditions}, \\ u(0,\cdot,\cdot) = u_0(\cdot,\cdot) \text{ and } v(0,\cdot,\cdot) = v_0(\cdot,\cdot) \text{ Dirichlet initial conditions}. \end{cases} \tag{3.4}$$

Remark 3.1. The well posedness of the problem (3.4) is established in [24] for 1-D reaction diffusion system, we have the same result for 2-D system, and we have:

For each $\varphi \in X_\Lambda$, (3.4) has a unique mild solution $z(t) = z(\varphi, t) \in X_\Lambda$ and a classical solution $U(t,x,y) = [z(t)](x,y)$. Moreover, the set X_Λ is positively invariant under the flow $\Psi_t(\varphi) = z(\varphi,t)$ induced by (3.4), where

$$X_\Lambda = \left\{\varphi \in X : \varphi(x,y) \in \Lambda, (x,y) \in \overline{\Omega}\right\},$$
$$\Lambda = \left\{U = (u,v) \in \mathbb{R}^2 : u \geq 0, v \geq 0\right\}$$

and X is the Banach space $X_1 \times X_2$ ($X_1 = X_2 = \mathcal{C}(\overline{\Omega})$) and the associated norm is defined by

$$|\varphi| = |\varphi_1| + |\varphi_2|$$

for $\varphi = (\varphi_1, \varphi_2) \in X$.

Since $(x,y) \in \Omega = \{(x,y) : x^2 + y^2 < R^2\}$, we can write x and y in polar coordinates as follow $x = r\cos(\theta)$ and $y = r\sin(\theta)$ and the domain of definition becomes $\mathcal{D} = \{(r,\theta) : 0 < r < R,\ 0 \leq \theta < 2\pi\}$, where $r = \sqrt{x^2+y^2}$ and $\tan(\theta) = \frac{y}{x}$. Without loss of generalities we also denote $u(t,x,y) = u(t, r\cos(\theta), r\sin(\theta)) = u(t,r,\theta)$ and $v(t,x,y) = v(t, r\cos(\theta), r\sin(\theta)) = v(t,r,\theta)$ which are the densities of prey and predators respectively in polar coordinates. Therefore the Laplacian operator in polar coordinates is given by:

$$\Delta_{r\theta} = \frac{\partial^2}{\partial r^2} + \frac{1}{r}\frac{\partial}{\partial r} + \frac{1}{r^2}\frac{\partial^2}{\partial \theta^2}.$$

Then the spatio-temporal system (3.4) in polar coordinates is written as follows:

$$\begin{cases} \dfrac{\partial u(t,r,\theta)}{\partial t} = \Delta_{r\theta} u(t,r,\theta) + f(u(t,r,\theta), v(t,r,\theta)) \text{ for } (r,\theta) \in \mathcal{D} \text{ and } t > 0, \\ \dfrac{\partial v(t,r,\theta)}{\partial t} = \delta \Delta_{r\theta} v(t,r,\theta) + g(u(t,r,\theta), v(t,r,\theta)) \text{ for } (r,\theta) \in \mathcal{D} \text{ and } t > 0, \\ \partial_r u(\cdot,r,\theta) = \partial_r v(\cdot,r,\theta) = 0 \text{ for } r = R \text{ Radial derivative}, \\ u(0,\cdot,\cdot) = u_0(\cdot,\cdot) \text{ and } v(0,\cdot,\cdot) = v_0(\cdot,\cdot) \text{ Dirichlet initial conditions}, \end{cases} \tag{3.5}$$

where $f(u,v) = u(1-u) - \frac{av}{u+e_1}u$ and $g(u,v) = b(1 - \frac{v}{u+e_2})v$.

Next, we will try to determine the possible steady states of the spatio-temporal reaction diffusion system (3.5).
A steady state (u_e, v_e) of Eq. (3.5) is a solution of the following system

$$\begin{cases} \Delta_{r\theta} u_e + u_e(1-u_e) - \dfrac{a v_e}{u_e + e_1} u_e = 0, \\ \delta \Delta_{r\theta} v_e + b\left(1 - \dfrac{v_e}{u_e + e_2}\right) v_e = 0, \end{cases} \tag{3.6}$$

then (u_e, v_e) is also an equilibrium point for (1.4).

By a simple computation, the trivial steady states are in the following forms: $E_0 = (0, 0)$, $E_1 = (1, 0)$ and $E_2 = (0, e_2)$.

Let $\mathbb{R}^2_+ = \{(u, v) \in \mathbb{R}^2, u_0 \geq 0, v_0 \geq 0\}$. The following result gives the positivity of solutions starting in the positive cone $int(\mathbb{R}^2_+) = \{(u, v) \in \mathbb{R}^2, u_0 > 0, v_0 > 0\}$.

Theorem 3.1. *Let Γ be the set defined by*

$$\Gamma = \{(u, v) \in \mathbb{R}^2_+,\ 0 \leq u \leq 1,\ 0 \leq v \leq 1 + e_2\}.$$

(i) *The set Γ is positively invariant region.*
(ii) *All solutions of (3.4) initiating in Γ are ultimately bounded with respect to $\mathbb{R}^2_+$ and eventually enter the attracting set Γ.*

Proof.

(i) Let $(u(0), v(0)) \in \Gamma$, since $int(\mathbb{R}^2_+)$ is invariant for the system (2.2) (see Lemma 5 [17]), then the solution $(u(t), v(t))$ with initial condition $(u(0), v(0))$ remains positive and for all $t \geq 0$, $u(t) \leq 1$ and $v(t) \leq 1 + e_2$ and Γ is invariant. For more details see [17].

(ii) From Eq. $(3.4)_1$, we have

$$\begin{cases} \dfrac{\partial u(t, r, \theta)}{\partial t} = \Delta_{r\theta} u + u(1-u), \\ \dfrac{\partial u(\cdot, R, \theta)}{\partial r} = 0, \\ u(0, r, \theta) = u_0(r, \theta) \leq u_{01} = \max\limits_{(r,\theta) \in \overline{\mathcal{D}}} u_0(r, \theta). \end{cases} \tag{3.7}$$

By the comparison principe, we have $u(t, x, y) \leq u_1 \leq 1$ where $u_1(t) = \frac{u_{01}}{u_{01} + (1-u_{01})e^{-t}}$ is a solution of the following ODE:

$$\begin{cases} \dfrac{du_1}{\partial t} = u_1(1 - u_1) \\ u_1(0) = u_{01} \leq 1 \end{cases} \tag{3.8}$$

Then

$$\limsup_{t \to +\infty} u_1(t) \leq 1$$

From Eq. $(3.4)_2$ and as $u(t, r, \theta) \leq 1$, we have

$$\begin{cases} \dfrac{\partial v(t, r, \theta)}{\partial t} = \delta \Delta_{r\theta} v + b\left(1 - \dfrac{v}{u + e_2}\right) v \leq \delta \Delta v + b\left(1 - \dfrac{v}{1 + e_2}\right) v, \\ \dfrac{\partial v(\cdot, r, \theta)}{\partial \eta} = 0 \text{ on } \partial\mathcal{D}, \\ v(0, r, \theta) = v_0(r, \theta) \leq v_{01} = \max\limits_{(r,\theta) \overline{\mathcal{D}}} v_0(r, \theta). \end{cases} \tag{3.9}$$

By the comparison principe, we have $v(t, r, \theta) \leq v_1 \leq 1$ where $v_1(t) = \frac{(1+e_2)v_{01}}{v_{01} + (1+e_2-v_{01})e^{-bt}}$ is a solution of the following ODE:

$$\begin{cases} \dfrac{du_1}{\partial t} = b\left(1 - \dfrac{v_1}{1 + e_2}\right) v_1, \\ v_1(0) = v_{01} \leq 1. \end{cases} \tag{3.10}$$

Then, we deduce that

$$\limsup_{t \to +\infty} v_1(t) \leq 1 + e_2,$$

which completes the proof. □

Theorem 3.2.

(i) *The equilibrium point $E_0 = (0, 0)$ is unstable.*
(ii) *The equilibrium point $E_1 = (1, 0)$ is unstable.*
(iii) *If $e_1 > ae_2$, then $E_2 = (0, e_2)$ is unstable and if $e_1 < ae_2$, then $E_2 = (0, e_2)$ is asymptotically stable.*

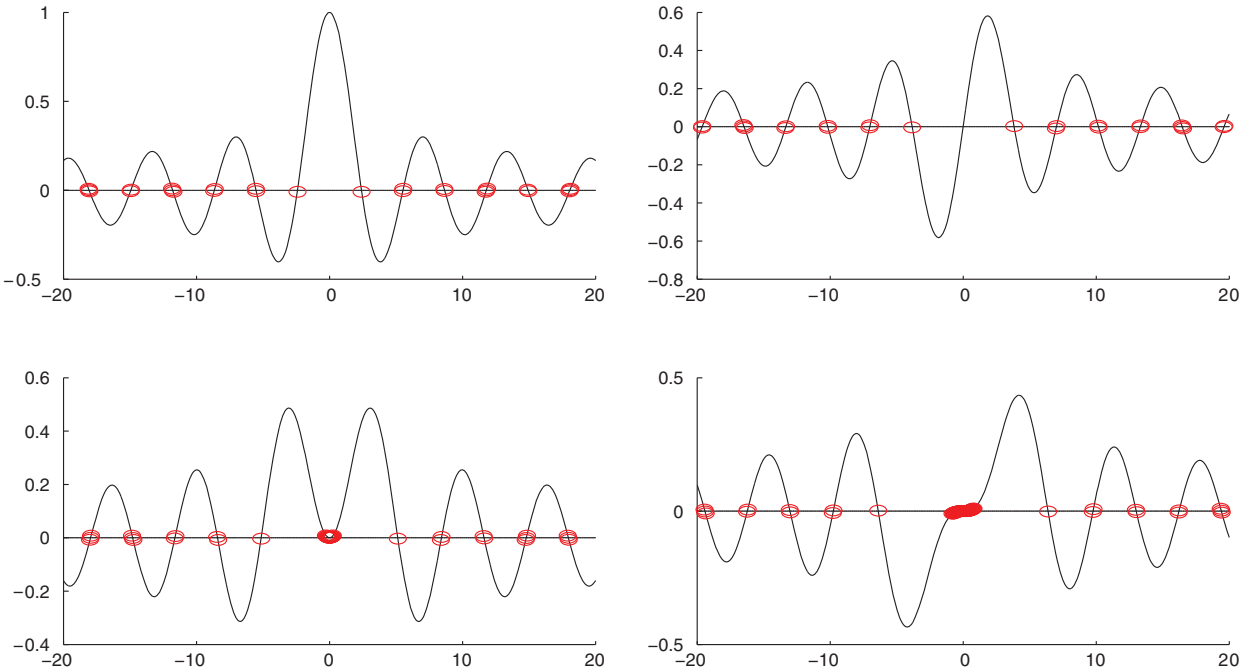

Fig. 1. Curves of Bessel functions of the first kind $J_i(x)$, $i = 0, 1, 2, 3$ and their roots in red circle. (For interpretation of the references to color in this figure legend, the reader is referred to the web version of this article.)

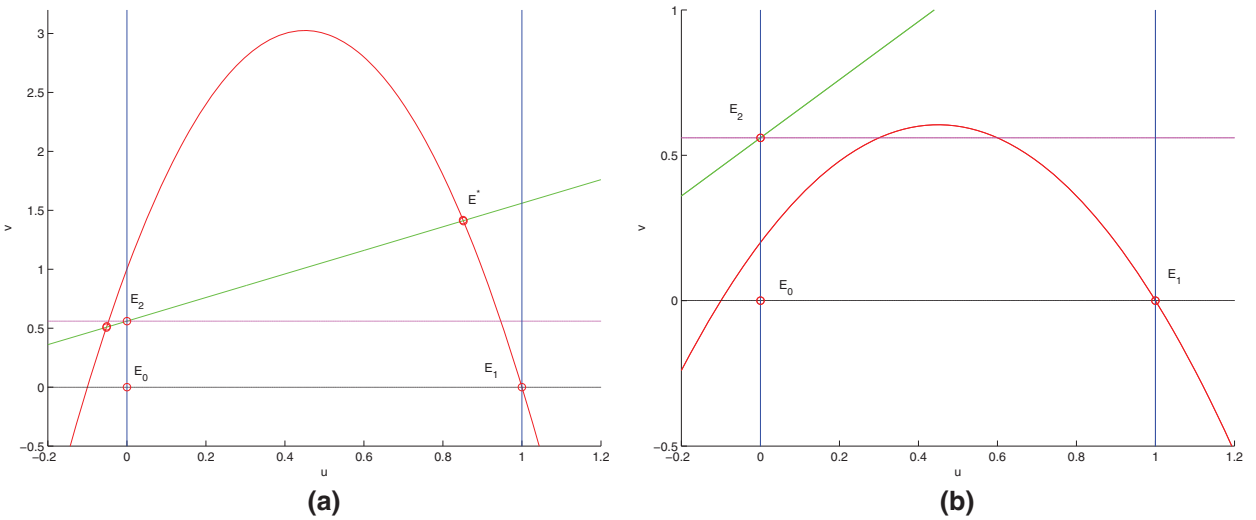

Fig. 2. Nullclines and possible equilibrium points of system (1.3) with $a = 0.1$; $e_1 = 0.1$; $e_2 = 0.56$ for subfigure (a) and $a = 0.5$; $e_1 = 0.1$; $e_2 = 0.56$ for subfigure (b).

Proof. See [9] (the existence of equilibrium points is illustrated in Fig. 2). □

Theorem 3.3. *Suppose $e_1 > ae_2$, then, system (3.5) have a unique non-trivial positive steady state $E^* = (u^*, v^*)$, where u^* is given in Eq. (2.3).*

If $a > \frac{1}{2(1+e_2)}$ and $0 \le e_1 \le e_{1+}$are satisfied, then, the non-trivial equilibrium point E^* is asymptotically stable.

Where

$$e_{1+} = -(a+1) + \sqrt{(a+1)^2 - 1 + 2a(1+e_2)}.$$

Proof. To study the asymptotic stability of the non-trivial steady state E^*, one needs to linearize system (3.5) around it. Let

$$(u(r,\theta,t), v(r,\theta,t)) = E^* + W(t,r,\theta) = E^* + (W_1(t,r,\theta), W_2(t,r,\theta))$$

and the linearized system is as follows:

$$\frac{\partial W}{\partial t} = D\Delta_{r\theta} W + MW \tag{3.11}$$

where $D = \begin{pmatrix} 1 & 0 \\ 0 & \delta \end{pmatrix}$ and $M = \begin{pmatrix} 1 - 2u^* - \frac{e_1(1-u^*)}{u^*+e_1} & -\frac{au^*}{u^*+e_1} \\ b & -b \end{pmatrix}$.

From the spectral problem presented in the Section 2.2, the solutions of Eq. (3.11) take the following form

$$W(t, r, \theta) = \sum_{n=0}^{+\infty} h_n(t)\phi_n^{\lambda_{nm}}(r, \theta)$$

where $\phi_n^{\lambda_{nm}}(r, \theta)$ is the eigenfunction of $\Delta_{r\theta}$ of λ_{nm} defined in (2.11) and $h_n(t) \in \mathbb{R}^2$.

From Eq. (3.11), we have

$$\frac{dh_n(t)}{dt} = N_n h_n(t)$$

where $N_n = M - \lambda_{nm} D$ and the characteristic equations associated to N_n is given by:

$$\begin{aligned}
\det(\gamma I - N_n) &= \left(\gamma - 1 + 2u^* + \frac{e_1(1-u^*)}{u^*+e_1} - \lambda_{nm}\right)(\gamma + b + \lambda_{nm}\delta) + b\frac{au^*}{u^*+e_1}, \\
&= \gamma^2 + \gamma\left(-1 + 2u^* + \frac{e_1(1-u^*)}{u^*+e_1} + \lambda_{nm} + b + \lambda_{nm}\delta\right) \\
&\quad + (b + \lambda_{nm}\delta)\left(-1 + 2u^* + \frac{e_1(1-u^*)}{u^*+e_1} + \lambda_{nm}\right) + b\frac{au^*}{u^*+e_1}, \\
&= \gamma^2 + \gamma G + H,
\end{aligned}$$

where

$$G = -1 + 2u^* + \frac{e_1(1-u^*)}{u^*+e_1} + \lambda_{nm} + b + \lambda_{nm}\delta$$

and

$$H = (b + \lambda_{nm}\delta)\left(-1 + 2u^* + \frac{e_1(1-u^*)}{u^*+e_1} + \lambda_{nm}\right) + b\frac{au^*}{u^*+e_1}.$$

Then

$$\gamma_{\pm} = \frac{-G \pm \sqrt{G^2 - 4H}}{2}.$$

Therefore, $\mathrm{Re}(\gamma_{\pm})$ is negative if $G > 0$ and $H > 0$. As $\lambda_{nm} = (\frac{\alpha_{nm}}{R})^2 > 0$ (see Section 2.2), $\delta > 0$ and $b > 0$, we need only to have $-1 + 2u^* + \frac{e_1(1-u^*)}{u^*+e_1} > 0$ which imply that $2u^* - 1 + e_1 \geq 0$. From formula of u^* given in (2.3), we have $a > \sqrt{\Delta}$ where Δ is defined by $\Delta = (a + e_1 - 1)^2 + 4(e_1 - ae_2)$. A simple computation gives us

$$\Delta - a^2 = e_1^2 + e_1(2a + 2) - 2a(1 + e_2) + 1$$

which is negative if $e_1 \leq e_{1+} = -(a + 1) + \sqrt{(a + 1)^2 - 1 + 2a(1 + e_2)}$, and we must have $e_{1+} > 0$ which is satisfied if $a > \frac{1}{2(1+e_2)}$.

Then, $\mathrm{Re}(\gamma_{\pm}) < 0$ for $e_1 \leq e_{1+}$ and we deduce the results. □

4. Global stability of the non-trivial steady state

In this section, we study the global stability of the homogeneous non-trivial steady state $E^* = (u^*, v^*)$.

Theorem 4.1. *Let*

(i) $0 < a < 1 \leq e_1 \leq e_2$ *and* $ae_2 < e_1$.

If (i) is satisfied, then the steady state E^* is globally asymptotically stable for system (3.5).

Proof. The proof is based on a positive definite Lyapunov function.

The hypothesis $0 < a < 1$ ensures that $ae_2 < e_2$ and $ae_2 < e_1$ ensures the existence of the non-trivial positive steady state E^*. Since $\mathcal{D} = \{(r, \theta) : 0 < r < R,\ 0 < \theta < 2\pi\}$, we denote $\int_{\mathcal{D}} f(\rho)d\rho = \int_0^R \int_0^{2\pi} f(r, \theta)d\theta dr$ and $V(u, v) = h_1(u) + h_2(v)$, where $h_1(u) = \int_{u^*}^{u} \frac{(\eta - u^*)(\eta + e_1)}{a\eta(\eta + e_2)}d\eta$ and $h_2(v) = \frac{u^* + e_2}{bv^*}\int_{v^*}^{v} \frac{\eta - v^*}{\eta}d\eta$. □

Remark 4.1. Note that V is a Lyapunov function associated to system (3.5) without diffusion see [2,8], in this case its demonstrated that the steady state E^* is globally asymptotically stable under the condition $e_1 \geq 1$. Also in 1-D reaction diffusion system its proved that the steady state E^* of system (3.5) is globally asymptotically stable under the condition $e_2 \geq e_1 \geq 1$ (see [4]). In the

next we will prove the global stability of E^* in 2-D reaction diffusion system (3.5) by adapting the method presented in [7] to our situation.

Let

$$\begin{aligned} W(u,v) &= \int_{\mathcal{D}} V(u(t,\rho),v(t,\rho))d\rho, \\ &= \int_{\mathcal{D}} h_1(u(t,\rho))d\rho + \int_{\mathcal{D}} h_2(u(t,\rho))d\rho. \end{aligned}$$

W is positive for all $(u,v)\in\mathbb{R}^2_{*+}$ and $W(u^*,v^*)=0$. By differentiating W with respect to time t, we have:

$$\begin{aligned} \frac{dW}{dt} &= \int_{\mathcal{D}} \left(\frac{\partial V}{\partial u}\frac{\partial u}{\partial t} + \frac{\partial V}{\partial v}\frac{\partial v}{\partial t} \right) d\rho, \\ &= \int_{\mathcal{D}} \left(\frac{\partial V}{\partial u}\left(\Delta u + f(u,v)\right) + \frac{\partial V}{\partial v}\left(\delta\Delta v + g(u,v)\right) \right) d\rho, \\ &= \int_{\mathcal{D}} \left(\frac{\partial V}{\partial u}\Delta u + \delta\frac{\partial V}{\partial v}\Delta v \right) d\rho + \int_{\mathcal{D}} \left(\frac{\partial V}{\partial u}f(u,v) + \frac{\partial V}{\partial v}g(u,v) \right) d\rho, \\ &= \int_{\mathcal{D}} \left(\frac{\partial V}{\partial u}\Delta u + \delta\frac{\partial V}{\partial v}\Delta v \right) d\rho + \int_{\mathcal{D}} \dot{V}d\rho, \end{aligned}$$

where $\dot{V} = \frac{\partial V}{\partial t}$.

From Green's identity we get:

$$\begin{aligned} \int_{\mathcal{D}} \frac{\partial V}{\partial u}\Delta u d\rho &= \int_{\partial\mathcal{D}} \frac{\partial V}{\partial u}\frac{\partial u}{\partial \eta} - \int_{\mathcal{D}} \nabla\frac{\partial V}{\partial u}\nabla u d\rho, \\ &= -\int_{\mathcal{D}} \nabla\frac{\partial V}{\partial u}\nabla u d\rho \end{aligned}$$

and

$$\begin{aligned} \int_{\mathcal{D}} \frac{\partial V}{\partial v}\Delta v d\rho &= \int_{\partial\mathcal{D}} \frac{\partial V}{\partial v}\frac{\partial v}{\partial \eta} - \int_{\mathcal{D}} \nabla\frac{\partial V}{\partial v}\nabla v d\rho, \\ &= -\int_{\mathcal{D}} \nabla\frac{\partial V}{\partial v}\nabla v d\rho, \end{aligned}$$

where $\nabla_{r\theta}u = \left(\frac{\partial u}{\partial r}, \frac{1}{r}\frac{\partial u}{\partial \theta}\right)$.

As $V(u,v) = h_1(u) + h_2(v)$ is written in a separable form and

$$h_1''(u) = \frac{1}{a}\left((u^* + e_2 - e_1)u^2 + 2e_1u^*u + e_1e_2u^* \right)$$

and

$$h_2''(v) = \frac{u^* + e_2}{bv^*}\cdot\frac{v^*}{v^2} \geq 0.$$

Then, under the condition $e_2 > e_1$ we have $h_1'' \geq 0$.

Therefore the matrix

$$\begin{pmatrix} \frac{\partial^2 V}{(\partial u)^2} & \frac{\partial^2 V}{\partial u \partial v} \\ \frac{\partial^2 V}{\partial v \partial u} & \frac{\partial^2 V}{(\partial v)^2} \end{pmatrix}$$

is positive definite and we have

$$\int_{\mathcal{D}} \left(\frac{\partial V}{\partial u}\Delta u + \delta\frac{\partial V}{\partial v}\Delta v \right) d\rho \leq 0.$$

As $\dot{V} \leq 0$ for $e_1 \geq 1$, we deduce that

$$\frac{dW}{dt} \leq 0 \text{ for } 0 < a < 1 \leq e_1 \leq e_2.$$

Then, we have the result.

5. Diffusion driven instability

By setting

$$Z = \begin{pmatrix} u-u^* \\ v-v^* \end{pmatrix} \varphi(r,\theta) e^{\lambda t + ikr},$$

where k is the wave number and $\varphi(r,\theta)$ is a eigenfunction of the Laplacian operator on a disc domain defined in Section 2.2 with zero flux boundary, i.e.:

$$\begin{cases} \Delta_{r\theta}\varphi = -k^2\varphi, \\ \varphi_r(R,\theta) = 0. \end{cases}$$

Then by linearizing around (u^*, v^*), we have the following equation:

$$\frac{dZ}{dt} = AZ + D\Delta Z \tag{5.1}$$

where

$$A = \begin{pmatrix} f_u & f_v \\ g_u & g_v \end{pmatrix} = \begin{pmatrix} 1 - 2u^* - \dfrac{e_1(1-u^*)}{e_1+u^*} & -\dfrac{au^*}{e_1+u^*} \\ b & -b \end{pmatrix}, \; D = \begin{pmatrix} 1 & 0 \\ 0 & \delta \end{pmatrix}$$

and
$f_u = \frac{\partial}{\partial u} f(u^*, v^*)$, $f_v = \frac{\partial}{\partial v} f(u^*, v^*)$, $g_u = \frac{\partial}{\partial u} g(u^*, v^*)$, $g_v = \frac{\partial}{\partial v} g(u^*, v^*)$.

Theorem 5.1. *Suppose that $\delta < \delta_c$ $b + e_1 > 1$ or $0 < u^* < \alpha_1$ or $\alpha_2 < u^*$, so that $E^* = (u^*, v^*)$ is asymptotically stable for system (3.5) without diffusion.*

Then, $E^* = (u^*, v^*)$ is unstable for system (3.5) if $\delta > \delta_c$ where

$$\delta_c = \frac{-(2f_v g_u - f_u g_v) + 2\sqrt{f_v g_u (f_v g_u - f_u g_v)}}{f_u^2}.$$

If we consider the ODE system of (3.5) (without diffusion), the stability of $E^* = (u^*, v^*)$ is recalled in Section 3.

Consider now the system with diffusion (3.5). By substituting Z by $\varphi e^{\lambda t}$ in Eq. (5.1) and canceling $e^{\lambda t}$, we get:

$$\lambda\varphi = (A - Dk^2\varphi) \tag{5.2}$$

Since we require φ to be a non trivial solution of Eq. (5.2), therefore λ is a zero of the following characteristic equation defined by

$$\Delta(k^2) = \det(\lambda I_2 - A + k^2 D) = 0 \tag{5.3}$$

and the solution λ is a function of the numberwave k in this case we write $\lambda = \lambda(k)$.

By computation, we have the expression of the characteristic equation $\Delta(k^2)$:

$$\Delta(k^2) = \lambda^2 + B(k^2)\lambda + C(k^2), \tag{5.4}$$

where

$$B(k^2) = k^2(1+\delta) - \mathrm{tr}(A)$$

and

$$C(k^2) = \delta k^4 - (\delta f_u + g_v)k^2 + \det(A).$$

Remark 5.1. For $k^2 = 0$, the characteristic equation is written as: $\Delta(k^2 = 0) = \Delta = \lambda^2 + B(0)\lambda + C(0)$, where $B(k^2 = 0) = -\mathrm{tr}(A)$ and $C(k^2 = 0) = \det(A)$. Which coincides with the characteristic equation of the Eq. (5.1) without diffusion and the stability of (u^*, v^*) is studied in [2].

The corresponding eigenvalues of the characteristic Eq. (5.4) are:

$$\lambda_{\pm}(k) = \frac{-B(k^2) \pm \sqrt{(B(k^2))^2 - 4C(K^2)}}{2}.$$

Next, we will work under the conditions of Turing instability which are as follows (see [19]):

$$B(0) = -\mathrm{tr}(A) = -(f_u + g_v) < 0, \tag{5.5}$$

$$C(0) = \det(A) = f_u g_v - f_v g_u > 0, \tag{5.6}$$

$$\delta f_u + g_v > 0, \tag{5.7}$$

$$(\delta f_u + g_v)^2 - 4\delta \det(A) > 0. \tag{5.8}$$

The imaginary part of $\lambda(k)$ is also important, because it allows the perturbation to be periodic in time.

The case when $\mathrm{Im}(\lambda(k_c)) = 0$ is called Turing instability and corresponds to the onset of patterns periodic in space and stationary in time.

On the other hand, for $\mathrm{Im}(\lambda(k_c)) \neq 0$ the instability is Hopf type. This corresponds to instability leading to a limit cycle oscillations in time.

Remark 5.2. Two cases of Hopf instability:

- $k_c = 0$ (and $\mathrm{Im}(\lambda(0)) \neq 0$), the homogenous Hopf instability case. The instability leads to (spatially homogenous) time oscillations.
- $k_c \neq 0$ (and $\mathrm{Im}(\lambda(k_c)) \neq 0$), the wave instability. The instability leading to traveling waves happens.

Since $A(k) = A(-k)$ that imply symmetry that is $\lambda(k) = \lambda(-k)$ and if the k_c exits also $-k_c$ exists.

As $A(k)$ is 2×2 matrix, there exist two different eigenvalues $\lambda(k)$ for each wave number k.

Remark 5.3. If $\det(A(k)) > 0$ and $\mathrm{tr}(A(k)) < 0$, we have $\mathrm{Re}(\lambda_{\pm}(k)) < 0\ \forall k$, which imply the nontrivial equilibrium point is stable.

1. There exits k_c such that $\det(A(k_c)) = C(k_c^2) = 0$ and $\mathrm{tr}(A(k_c)) = -B(k_c^2) < 0$ whereas $\det(A(k)) > 0$ and $\mathrm{tr}(A(k)) < 0 \forall k \neq k_c$.
2. There exits k_c such that $\det(A(k_c)) > 0$ and $\mathrm{tr}(A(k_c)) = 0$ whereas $\det(A(k)) > 0$ and $\mathrm{tr}(A(k)) < 0 \forall k \neq k_c$.

We call the two conditions instability threshold conditions. At these threshold conditions the system is critical and one or more eigenvalues with zero real part called critical eigenvalues.

In case 1: both eigenvalues are real. $\lambda_+(k_c) = 0$ and $\lambda_-(k_c) < 0$ imply Turing instability and denote k_c by k_T.

In case 2: $\lambda_+(k_c) = iw_c$ and $\lambda_-(k_c) = -iw_c$ where $w_c = \sqrt{\det(A(k_c))}$ imply Hopf instability with critical wavenumber k_c and critical frequency w_c.

Remark 5.4. If $k_c = 0$, an homogenous Hopf instability appears.

If $k_c \neq 0$, a wave instability arises, denote $k_c = k_W$.

For the steady state E^* to be unstable to spatial disturbances, we need $\mathrm{Re}(\lambda(k))$ to be strictly positive for some $k \neq 0$. Then, we have $\mathrm{Re}(\lambda(k)) > 0$ if $B(k^2) < 0$ or $C(k^2) < 0$ for some $k \neq 0$. As $\mathrm{tr}(A) = f_u + g_v < 0$ and $k^2(1+\delta) > 0$, we have $B(k^2) > 0$ for all k (see Fig. 3) and the only choice for $\mathrm{Re}(\lambda(k)) > 0$ is $C(k^2) < 0$ for some $k \neq 0$ (see Fig. 4).

To know the sign of $C(k^2)$, we need to study their variations with respect to the wavenumber k^2. By differentiation

$$C'(k^2) = 2\delta k^2 - (\delta f_u + g_v)$$

and

$$C'(k^2) = 0 \Longleftrightarrow k = k_{\min} = \sqrt{\frac{\delta f_u + g_v}{2\delta}}.$$

Then,

$$C_{\min} = C(k_{\min}^2) = \det(A) - \frac{(\delta f_u + g_v)^2}{4\delta}.$$

If $\det(A) < \frac{(\delta f_u + g_v)^2}{4\delta}$, by continuity property there exists $k^2 \neq 0$ such that $C(k^2) < 0$.

To obtain bifurcation in which $C_{\min} = 0$ that is $\det(A) = \frac{(\delta f_u + g_v)^2}{4\delta}$, there exists a critical value δ_c of the diffusion coefficient delta which is a solution of the equation:

$$\delta^2 f_u^2 + 2\delta(2f_v g_u - f_u g_v) + g_v^2 = 0. \tag{5.9}$$

If we consider δ as a parameter of bifurcation from Eq. (5.9), we compute the values of δ_c:

$$\delta_{c1,2} = \frac{-(2f_v g_u - f_u g_v) \pm \sqrt{(2f_v g_u - f_u g_v)^2 - f_u^2 g_v^2}}{f_u^2}. \tag{5.10}$$

We note δ_c by δ_T (see Fig. 5) given by

$$\delta_T = b\frac{-(2f_v + f_u) \pm \sqrt{(2f_v + f_u)^2 - f_u^2}}{f_u^2}. \tag{5.11}$$

As $C(k_c^2) = 0$, $B(k_c^2) < 0$, $C(k^2) < 0$ and $B(k^2) < 0$ for all $k^2 \neq k_c^2$ (see Remark 5.3). Then the critical value k_c of the wavenumber k is given as:

$$k_T^2 = \frac{\delta_T f_u - b}{2\delta_T}$$

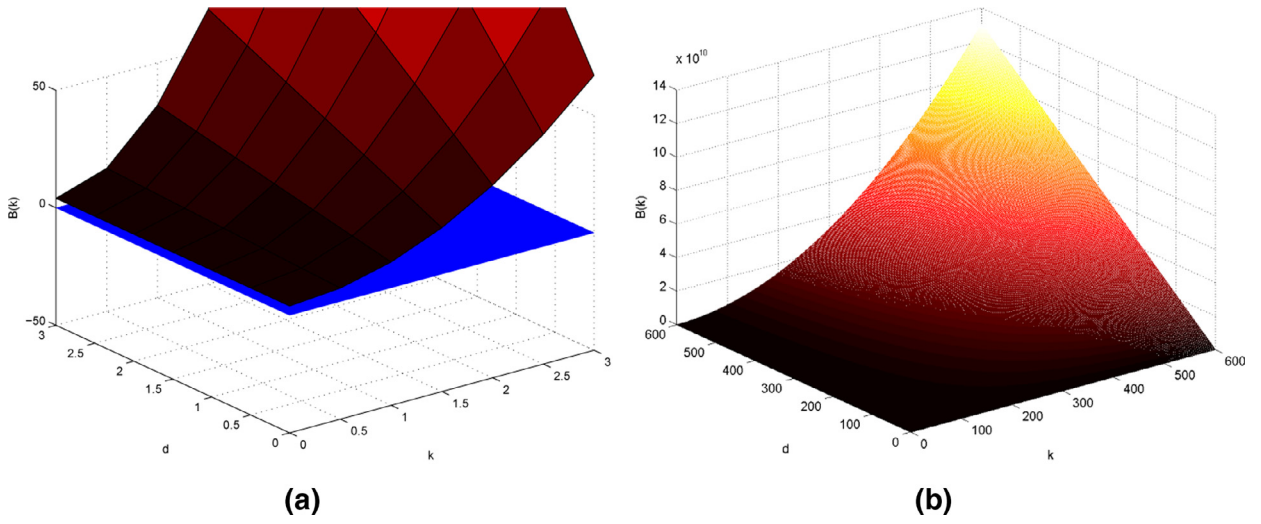

Fig. 3. Surfaces in 3-D representing the positivity of the function $B(k)$ with respect to variables k and blue surface in subfigure (a) is the vanishing plane. Subfigure (a) is a zoom of the subfigure (b). (For interpretation of the references to color in this figure legend, the reader is referred to the web version of this article.)

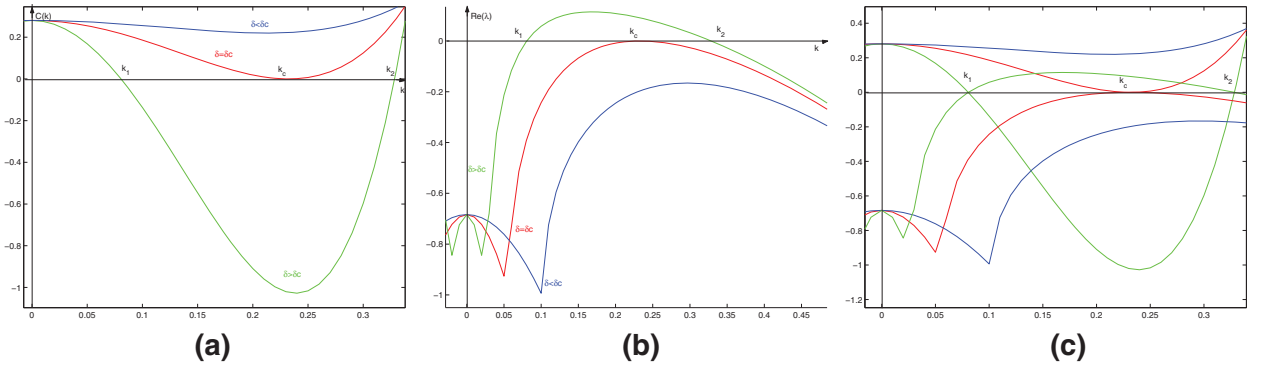

Fig. 4. $C(k^2)$ function (a) and $\mathrm{Re}(\lambda(k))$ (b) with respect to the wavenumber k^2. From Fig. 4, we observe that there exist two values k_i^2, $i = 1, 2$ of k^2 such that $C(k^2) < 0$ and $\mathrm{Re}(\lambda(k)) > 0$ for $k_1^2 < k^2 < k_2^2$ we call $]k_1^2, k_2^2[$ the region of wavenumbers of unstable modes. Blue curves are plotted for $\delta > \delta_T$ and the red curves for $\delta = \delta_T$ and green lines for $\delta < \delta_T$. (c) is plotted for comparison we see that $C(k^2) = \mathrm{Re}(\lambda(k)) = 0$ at k_i^2, $i = 1, 2$. (For interpretation of the references to color in this figure legend, the reader is referred to the web version of this article.)

and the wavelength is given by

$$w_T = \frac{2\pi}{k_T} = 2\pi\sqrt{\frac{2\delta_T}{\delta_T f_u - b}}.$$

To define the region of wavenumbers of unstable modes one needs to solve the equation $C(k^2) = 0$ (see Fig. 4). Then, we have

$$k_1^2 = \frac{1}{2\delta}\left((\delta f_u + g_v) - \sqrt{(\delta f_u + g_v)^2 - 4\delta\det(A)}\right),$$
$$k_2^2 = \frac{1}{2\delta}\left((\delta f_u + g_v) + \sqrt{(\delta f_u + g_v)^2 - 4\delta\det(A)}\right).$$

Remark 5.5.

(i) The first condition of Turing ensures that $B(k^2) < 0$, the second allows us to solve the equations $\det(A) = \frac{(\delta f_u + g_v)^2}{4\delta}$, the third one gives us the positivity of $k_T^2 = \frac{\delta_c f_u - b}{2\delta_c}$. The last conditions ensure the positivity of $k_i^2; i = 1, 2$.

(ii) If we consider b (see Fig. 5) as a parameter of bifurcation, from Eq. (5.9) we have

$$\delta^2 f_u^2 + 2\delta(2f_v g_u - f_u g_v) + g_v^2 = b^2 + 2b\delta(2f_v + f_u) + \delta^2 f_u^2 = 0 \tag{5.12}$$

and

$$b_T = \delta\left(-(2f_v + f_u) \pm \sqrt{(2f_v + f_u)^2 - f_u^2}\right)$$

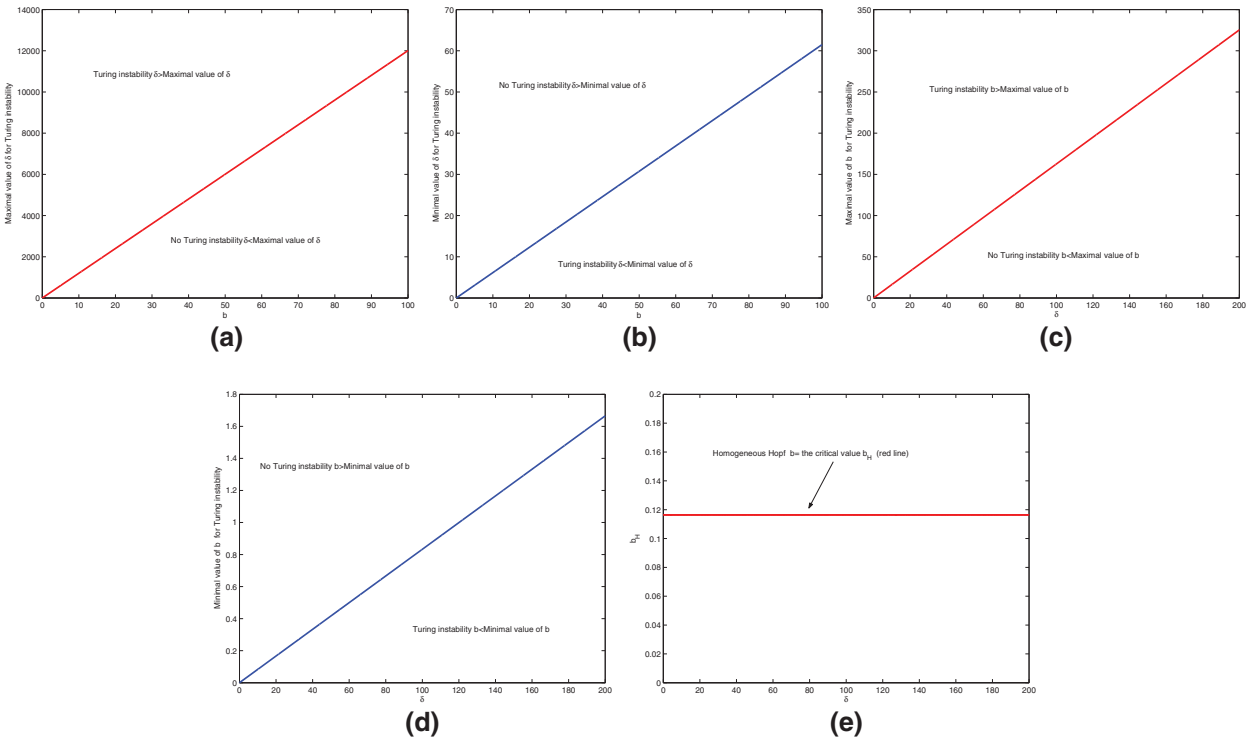

Fig. 5. Curves of maximal and minimal critical values of δ vs b (a), (b) and b vs δ (c), (d) and the curve which gives the critical value b_H of homogeneous Hopf (e).

and

$$k_T^2 = \frac{\delta f_u - b_T}{2\delta}$$

and wavelength is:

$$w_T = \frac{2\pi}{k_T} = 2\pi\sqrt{\frac{2\delta}{\delta f_u - b_T}}.$$

The region of Turing instability and of homogeneous Hopf are illustrated in Fig. 5.

The violation of the first Turing conditions leads to the Hopf bifurcation, i.e., the onset of Hopf instability is (see Remarks 5.1 and 5.2)

$$\mathrm{tr}(A) = f_u - b \geq 0,$$

which gives us the Hopf critical value (which corresponds to the case when $k = 0$)

$$b_H = f_u = 1 - 2u^* - \frac{e_1(1-u^*)}{e_1 + u^*} \tag{5.13}$$

and the region of the Hopf instability is given by $b > b_H$ and the frequency of oscillations is

$$\mu_H = \sqrt{\det(A)} = \sqrt{b_H(f_u + f_v)} = \sqrt{b_H u^* \frac{2u^* + a + e_1 - 1}{u^* + e_1}} \tag{5.14}$$

and the wavelength is

$$w_H = \frac{2\pi}{\mu_H} = 2\pi\sqrt{\frac{1}{b_H u^*}\frac{u^* + e_1}{2u^* + a + e_1 - 1}}. \tag{5.15}$$

Proposition 5.1. *If*

$$\delta = \delta_\pm = \frac{-(2f_v + f_u) \pm \sqrt{(2f_v + f_u)^2 - f_u^2}}{f_u}$$

Then $b_T = b_H$.

Proof. As $b_H = f_u$ and $b_T = \delta(-(2f_v + f_u) \pm \sqrt{(2f_v + f_u)^2 - f_u^2})$, a simple computation leads to solve the second order equation in δ

$$f_u\delta^2 + 2\delta(2f_v + f_u) + f_u = 0.$$

Therefore, we deduce the result.

This result coincide with the numerical simulation given in Fig. 5(c)–(e), we observe that the horizontal line which present the critical value b_H of Hopf bifurcation in Fig. 5(d) intersect the lines which present the maximal and the minimal values of b_T at $\delta_\pm$. □

6. Numerical analysis

6.1. Numerical method

Eq. (3.5) is not defined at the origin $r = 0$, to avoid this singularity and to have the desired regularity the finite difference scheme [25] uses a uniform grid with some steady at the origin. This poles condition play the role as a boundary condition which is a necessary condition in the finite difference scheme. By discretization, the associated approximation of problem (3.5) takes the following form:

For $n = 1, \ldots, N$, with $N = \frac{T}{\Delta t}$, $i = 1, \ldots, P+1$, and $j = 1, \ldots, M+1$ find $\{u_{i,j}^n, v_{i,j}^n\}$ such that

$$\begin{cases} \partial_n u_{i,j}^n = \Delta_{r_i\theta_j} u_{i,j}^n + f(\overrightarrow{u_{i,j}^n}, \overrightarrow{u_{i,j}^{n-1}}), \\ \partial_n v_{i,j}^n = \delta \Delta_{r_i\theta_j} v_{i,j}^n + g(\overrightarrow{u_{i,j}^n}, \overrightarrow{u_{i,j}^{n-1}}), \end{cases} \tag{6.1}$$

with

$$\begin{cases} f(\overrightarrow{u_{i,j}^n}, \overrightarrow{u_{i,j}^{n-1}}) = u_{i,j}^{n-1} - u_{i,j}^{n-1}|u_{i,j}^{n-1}| - \dfrac{a v_{i,j}^{n-1}}{|u_{i,j}^{n-1}| + e_1} u_{i,j}^{n-1}, \\ g(\overrightarrow{u_{i,j}^n}, \overrightarrow{u_{i,j}^{n-1}}) = b v_{i,j}^{n-1} - \dfrac{b v_{i,j}^{n-1}}{|u_{i,j}^{n-1}| + e_2} v_{i,j}^{n-1}, \end{cases} \tag{6.2}$$

where $\overrightarrow{u_{i,j}^n} = (u_{i,j}^n, v_{i,j}^n)^T$ denotes the two-dimensional approximation at the point (r_i, θ_j, t_n) with $t_n = n\Delta t$. The approximations of the initial conditions are given as:

$$u_{i,j}^0 = u_0(r_i, \theta_j),\ v_{i,j}^0 = v_0(r_i, \theta_j).$$

We choose a grid which the grid points are integers in azimuthal direction and half-integer in radial direction and, that is

$$r_i = \left(i - \frac{1}{2}\right)\Delta r,\ \theta_j = (j-1)\Delta\theta, \tag{6.3}$$

where

$$\Delta r = \frac{2}{2P+1},\ \Delta\theta = \frac{2\pi}{M},$$

using the centered difference method to discretize the Laplacian operator, for $i = 2, \ldots, P$ and $j = 1, \ldots, M$ we have

$$\Delta_{r_i\theta_j} u_{i,j}^n \approx \frac{u_{i+1,j}^n + u_{i-1,j}^n - 2u_{i,j}^n}{\Delta r^2} + \frac{u_{i+1,j}^n - u_{i-1,j}^n}{2r_i\Delta r} + \frac{u_{i,j+1}^n + u_{i,j-1}^n - 2u_{i,j}^n}{r_i^2\Delta\theta^2}, \tag{6.4}$$

from the Neumann boundary conditions (the flow is zero on the edge)

$$\frac{u_{P+1,j}^n - u_{P,j}^n}{\Delta r} = 0, \tag{6.5}$$

so the numerical boundary values at $r = 1$, $u_{P+1,j}^n$ can be approximated by $u_{P,j}^n$, and $u_{i,0}^n = u_{i,M}^n$, $u_{i,1}^n = u_{i,M+1}^n$ since u is 2π periodic in θ. At $i = 1$, Eq. (6.4) becomes

$$\Delta_{r_1\theta_j} u_{1,j}^n \approx \frac{u_{2,j}^n + u_{0,j}^n - 2u_{1,j}^n}{\Delta r^2} + \frac{u_{2,j}^n - u_{0,j}^n}{2r_1\Delta r} + \frac{u_{1,j+1}^n + u_{1,j-1}^n - 2u_{1,j}^n}{r_1^2\Delta\theta^2}, \tag{6.6}$$

since $r_1 = \frac{\Delta r}{2}$, the term $u_{0,j}^n$ is simplified and the Eq. (6.6) becomes

$$\Delta_{r_1\theta_j} u_{1,j}^n \approx \frac{2(u_{2,j}^n - u_{1,j}^n)}{\Delta r^2} + \frac{u_{1,j+1}^n + u_{1,j-1}^n - 2u_{1,j}^n}{r_1^2\Delta\theta^2}. \tag{6.7}$$

We find the linear system is

$$\begin{pmatrix} B_1 & 0 \\ 0 & B_2 \end{pmatrix} \begin{pmatrix} \overrightarrow{U^n} \\ \overrightarrow{V^n} \end{pmatrix} = \begin{pmatrix} \overrightarrow{U^{n-1}} + \Delta t F \\ \overrightarrow{V^{n-1}} + \Delta t G \end{pmatrix}, \quad \text{where} \begin{pmatrix} B_1 = I + \Delta t L \\ B_2 = I + \delta \Delta t L \end{pmatrix}.$$

I is the identity matrix and L is the matrix of coefficients in polar coordinates, F and G are associated to the system (6.2).

$$\mathbf{L} = \begin{pmatrix} A-2D & D & 0 & \dots & 0 & D \\ D & \ddots & \ddots & \ddots & \ddots & 0 \\ 0 & \ddots & \ddots & \ddots & \ddots & \vdots \\ \vdots & \ddots & \ddots & \ddots & \ddots & 0 \\ 0 & \ddots & \ddots & \ddots & \ddots & D \\ D & 0 & \dots & 0 & D & A-2D \end{pmatrix},$$

where

$$\mathbf{A} = \begin{pmatrix} -2 & 1+\lambda_1 & 0 & \dots & \dots & 0 \\ 1-\lambda_2 & \ddots & \ddots & \ddots & \ddots & \vdots \\ 0 & \ddots & \ddots & 1+\lambda_i & \ddots & \vdots \\ \vdots & \ddots & 1-\lambda_i & \ddots & \ddots & \vdots \\ \vdots & \ddots & \ddots & \ddots & -2 & 1+\lambda_{P-1} \\ 0 & \dots & \dots & 0 & 1-\lambda_P & 1+\lambda_P \end{pmatrix}$$

and

$$\mathbf{D} = \begin{pmatrix} \beta_1 & 0 & \dots & \dots & \dots & 0 \\ 0 & \ddots & \ddots & \ddots & \ddots & \vdots \\ \vdots & \ddots & \beta_i & \ddots & \ddots & \vdots \\ \vdots & \ddots & \ddots & \ddots & \ddots & \vdots \\ \vdots & \ddots & \ddots & \ddots & \ddots & 0 \\ 0 & \dots & \dots & \dots & 0 & \beta_P \end{pmatrix}$$

with

$$\beta_i = \frac{1}{(i-0.5)^2 \Delta\theta^2}, \quad \lambda_i = \frac{1}{(i-0.5)}, \quad i = 1, \dots, P.$$

6.2. Numerical simulations

It is known that, the analytical solution of the coupled reaction diffusion system of predator prey type is not always possible. Thus we have to perform numerical simulations to solve them. The spatiotemporal system (3.5) is solved numerically in the disk $\Omega = \{(x, y) \in \mathbb{R}^2 : x^2 + y^2 < 400\}$. with $x = r\cos(\theta)$ and $y = r\sin(\theta)$. The Laplacian describing diffusion is calculated using finite difference schemes, that is, the derivatives are approached by differences over space steps (Δr) and an explicit Euler's method for the time integration with a time step size (Δt) with the zero-flux boundary conditions (homogeneous Neumann boundary conditions). In order to avoid numerical artifacts, the values of the time (Δt) and space steps (Δr and $\Delta\theta$) have been chosen sufficiently small. Satisfying the CFL (Courant–Friedrichs–Levy) stability criterion for diffusion equation, we introduce for $(3.5)_1$ (Resp. $(3.5)_2$):

$$\Delta t \leq \frac{r_i^2 \Delta r^2 \Delta\theta^2}{2r_i^2 \Delta\theta^2 + r_i \Delta r \Delta\theta^2 + 2\Delta r^2} \quad \left(\text{Resp. } \Delta t \leq \frac{r_i^2 \Delta r^2 \Delta\theta^2}{\delta(2r_i^2 \Delta\theta^2 + r_i \Delta r \Delta\theta^2 + 2\Delta r^2)} \right).$$

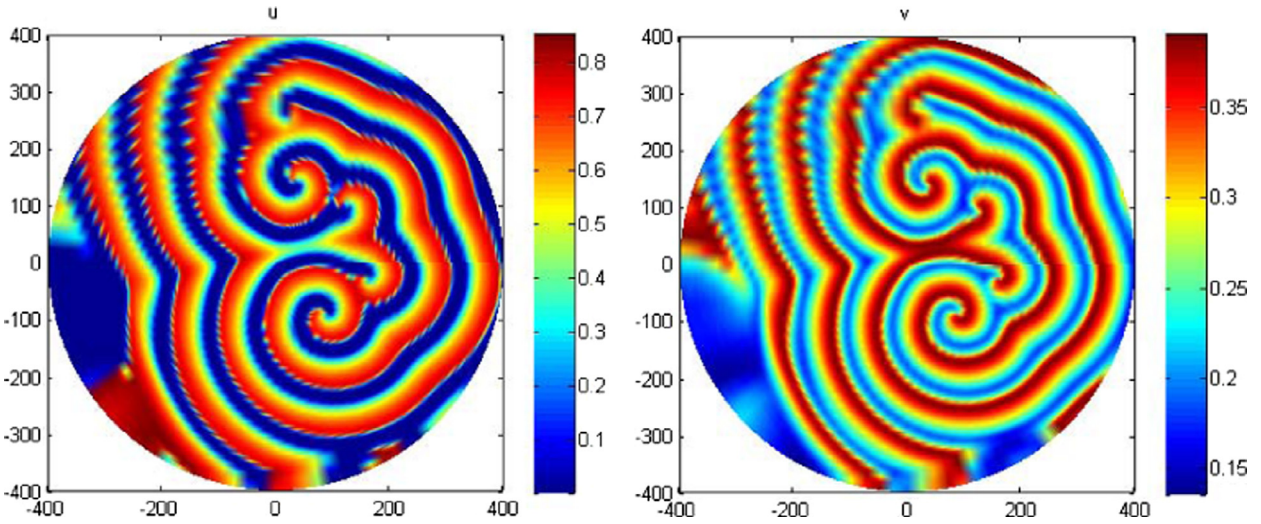

Fig. 6. Spatial spiral waves type distribution of species for fixed $\delta = 1$.

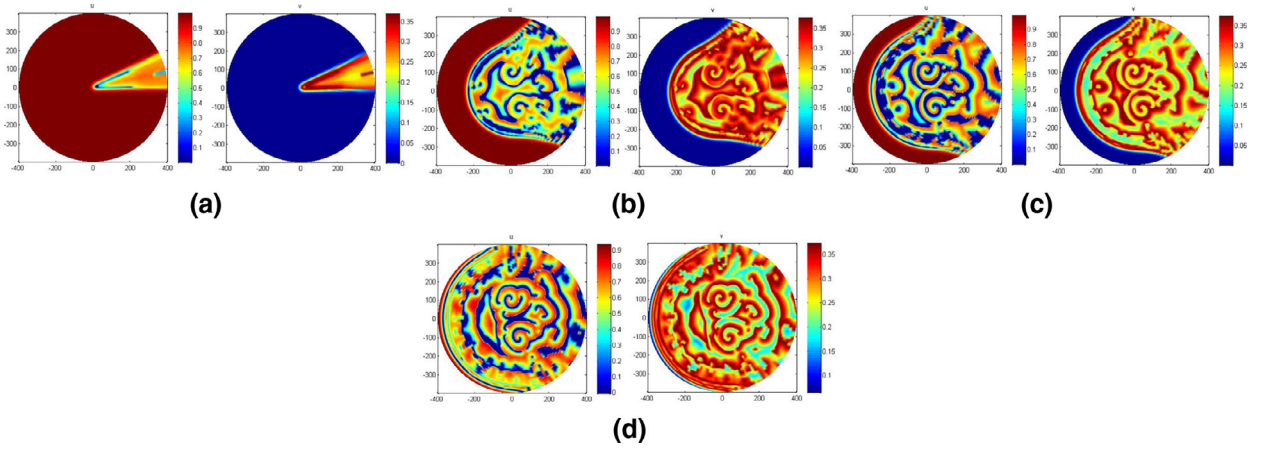

Fig. 7. Spatial distribution of species for fixed $\delta = 1$ and time varying.

The initial condition is a small perturbation in the vicinity of equilibrium point (u^*, v^*). These initial conditions have been chosen as,

$$u_0(r_i, \theta_j) = u^*((r_i\cos(\theta_j))^2 + (r_i\sin(\theta_j))^2) = u^* r_i^2 < 400, \tag{6.8}$$

$$v_0(r_i, \theta_j) = v^*((r_i\cos(\theta_j))^2 + (r_i\sin(\theta_j))^2) = v^* r_i^2 < 400. \tag{6.9}$$

Remark 6.1. From the conditions (6.8) and (6.9), it is clear that the disk center is (0, 0) and radius $R = 400$. Our initial perturbation can be improved to avoid confusion $((\cos(\theta))^2 + (\sin(\theta))^2 = 1)$. Via numerical simulation, we found that these conditions (6.8) and (6.9) are similar for these conditions (6.10) and (6.11) and the centre of the disk becomes (400, 400) and radius $R = 400$.

$$u_0(r_i, \theta_j) = u^*(((r_i\cos(\theta_j)) - 400)^2 + ((r_i\sin(\theta_j)) - 400)^2) < 800 \tag{6.10}$$

$$v_0(r_i, \theta_j) = v^*(((r_i\cos(\theta_j)) - 400)^2 + ((r_i\sin(\theta_j)) - 400)^2) < 800 \tag{6.11}$$

In the proposed model (3.5) through numerical simulations, different types of dynamics are observed. Firstly in Fig. 6, we observe the spatial distribution of spiral waves types for system (3.5) for time $t = 8000$. Next, we stop the simulation when the numerical solutions either reach a stationary state or show oscillatory behavior. The following time evolution of spatial distributions are observed (Figs. 7–9). The left figures are the evolution of the prey spatial distribution and the right ones are of the predators. After a while, the patterns show a behavior that does not seem to change its characteristics anymore, the stripes

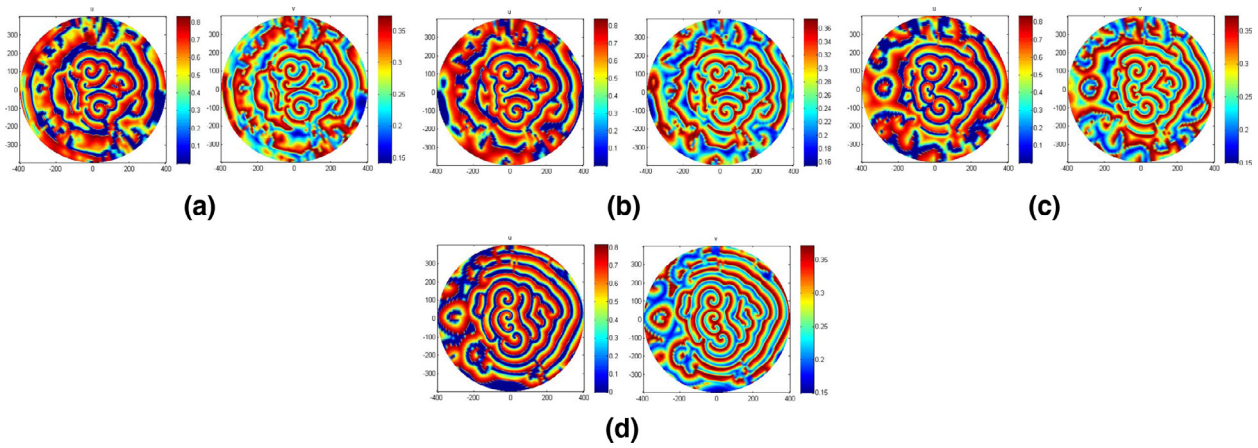

Fig. 8. Spatial distribution of species for fixed $\delta = 1$ and time varying.

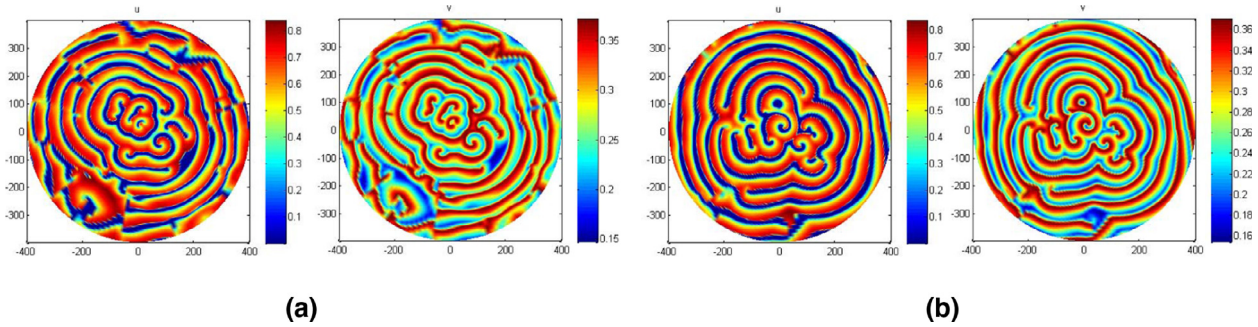

Fig. 9. Spatial distribution of species for $\delta = 1$.

Table 1
The values of parameters model, and the corresponding pictures of patterns are shown (Figs. 6–9).

Values of a	Values of b	Values of e_1	Values of e_2	Values of δ	Values of t	Contour pictures
1	0.002	0.2	0.1	1	8000	Fig. 6
1	0.01	0.2	0.1	1	500	Fig. 7(a)
1	0.01	0.2	0.1	1	4000	Fig. 7(b)
1	0.01	0.2	0.1	1	5000	Fig. 7(c)
1	0.01	0.2	0.1	1	6000	Fig. 7(d)
1	0.01	0.2	0.1	1	6500	Fig. 8(a)
1	0.01	0.2	0.1	1	7000	Fig. 8(b)
1	0.01	0.2	0.1	1	8000	Fig. 8(c)
1	0.01	0.2	0.1	1	10,000	Fig. 8(d)
1	0.01	0.2	0.1	1	20,000	Fig. 9(a)
1	0.01	0.2	0.1	1	30,000	Fig. 9(b)

spatial pattern arise. They grow with time and stripes pattern prevail over the whole domain at last (see Fig. 9(b)) and the dynamics of the system does not undergo any further changes. All values of the used parameters are summarized in Table 1.

In order to illustrate the phenomena caused by Hopf bifurcation numerically, we choose parameter values in system (3.5) as $a = 1, e_1 = 0.3, e_2 = 0.1, \delta = 1$ with small random perturbation of the stationary solution u^* and v^* of the spatially homogeneous system. We know that Hopf bifurcation occurs when $b > b_H = 0.0293$ (from (5.13)). Figs. 10 and 11, show snapshots of contour pictures of the time evolution of prey population in system (3.5) $b = 0.0295 > b_H$. However, it is a little bit hard to observe an oscillatory phenomenon arising from Hopf bifurcation from these snapshots. In addition, we can calculate numerically that the frequency of the periodic oscillations in time $\mu_H = 0.12$ and the corresponding wave length $\omega_H = 52.35$. Also, it follows from (5.14) and (5.15) that the theoretical frequency of the periodic oscillations in time is $\mu_H = 0.1196$ and the corresponding wave length $\omega_H = 52.54$.

The Turing instability is dependent only upon the reaction rates (local interaction of species) and populations diffusion and not upon the geometry of the system. It cannot be expected if the diffusion term is absent. It can occur only if prey population

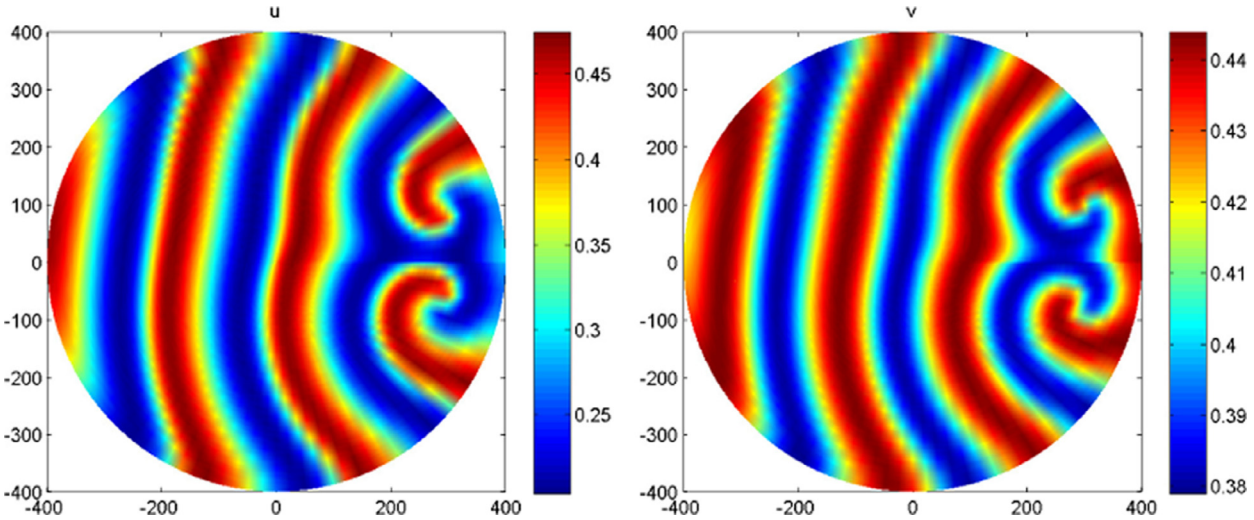

Fig. 10. Spatial distribution of prey predator species at $t = 50{,}000$ and $b = 0.0295$.

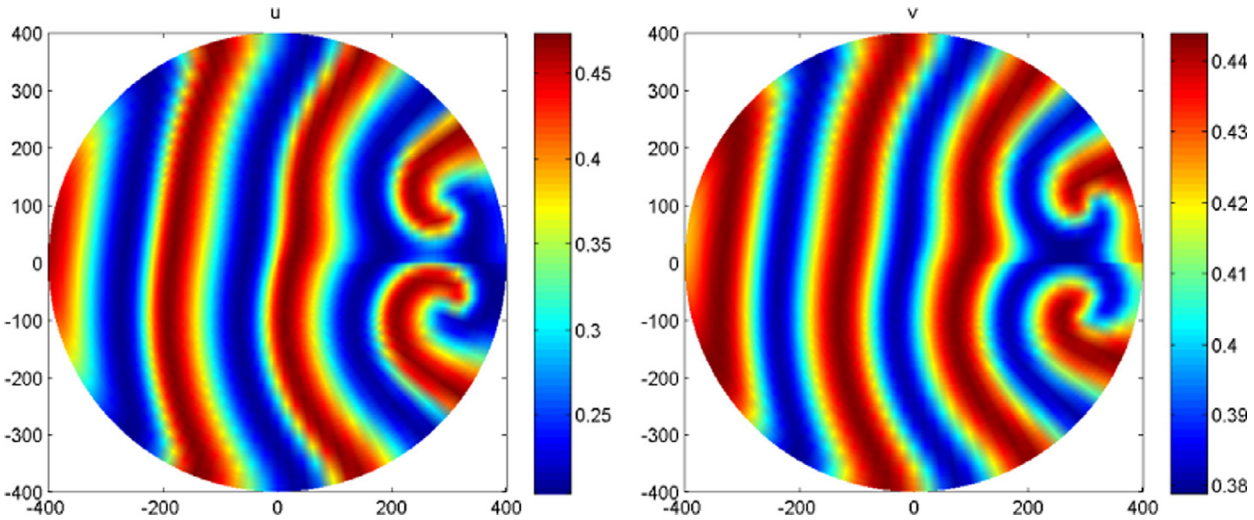

Fig. 11. Spatial distribution of prey predator species at $t = 70{,}000$ and $b = 0.0295$.

Table 2
The values of parameters model, and the corresponding pictures of patterns are shown (Fig. 12).

Values of a	Values of b	Values of e_1	Values of e_2	Values of δ	Values of t	Contour pictures
1	0.01	0.2	0.1	1.01	8000	Fig. 12(a)
1	0.01	0.2	0.1	1.1	8000	Fig. 12(b)
1	0.01	0.2	0.1	1.5	8000	Fig. 12(c)
1	0.01	0.2	0.1	1.52	8000	Fig. 12(d)
1	0.01	0.2	0.1	1.54	8000	Fig. 12(e)
1	0.01	0.2	0.1	1.55	8000	Fig. 12(f)
1	0.01	0.2	0.1	2.5	8000	Fig. 12(g)
1	0.01	0.2	0.1	5	8000	Fig. 12(h)

diffuses more slowly than predator one. We have studied numerically the effect of the diffusion coefficient δ on the pattern formation. All values of the used parameters are summarized in Table 2. The left column is the evolution of the prey spatial pattern and the right one is the predators. Fig. 12(a) (Resp. (b)–(e)) shows the evolution of the spatial pattern of the prey and predator at $t = 8000$ with small random perturbation of the stationary solution u^* and v^* of the spatially homogeneous system with $\delta = 1.01$ (Resp. $\delta = 1.1$, $\delta = 1.5$, $\delta = 1.52$, $\delta = 1.54$,). We see from these figures that the spotted and labyrinth patterns prevail in the whole domain. If we increase the diffusion coefficient $\delta = 1.55$ (Fig. 12(f)), the number of the spotted area in the

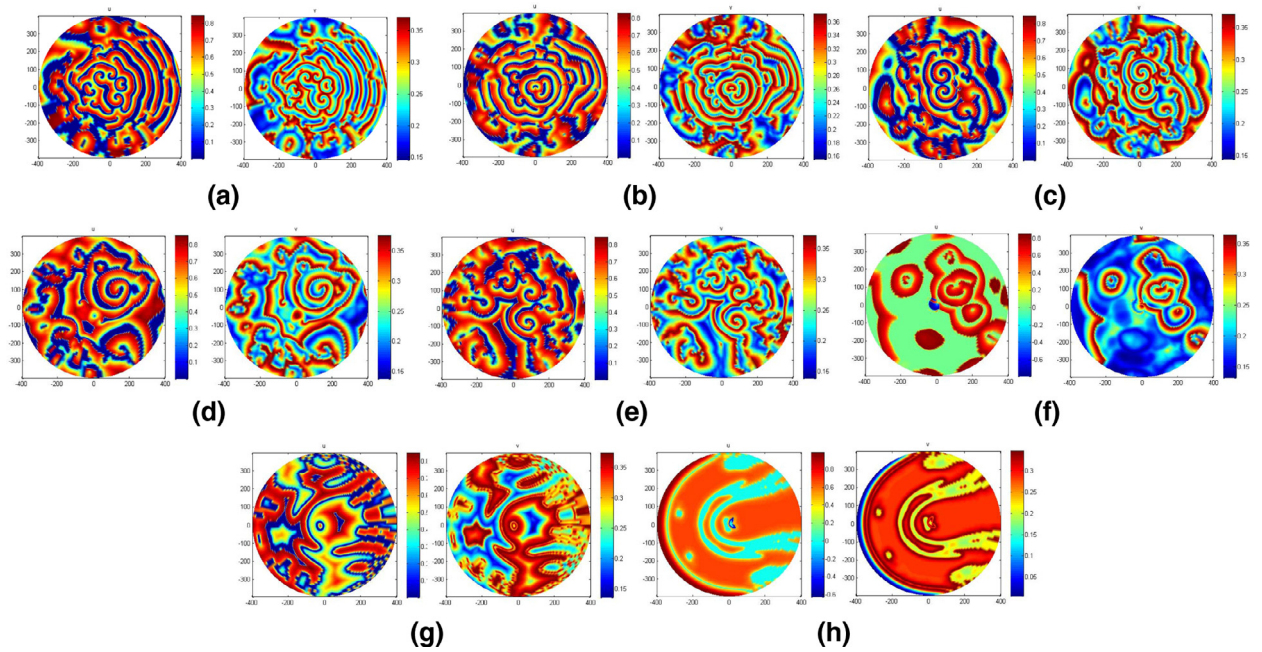

Fig. 12. Spatial distribution for fixed b and varying δ.

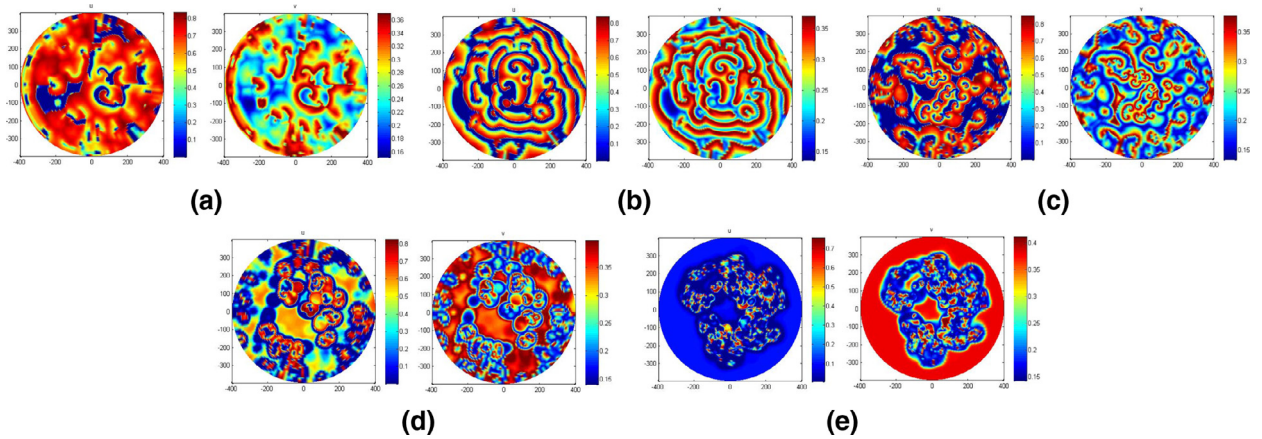

Fig. 13. Spatial distribution for fixed δ and varying b.

Table 3
The values of parameters model, and the corresponding pictures of patterns are shown (Fig. 13).

Values of a	Values of b	Values of e_1	Values of e_2	Values of δ	Values of t	Contour pictures
1	0.005	0.2	0.1	1.5	10,000	Fig. 13(a)
1	0.01	0.2	0.1	1.5	10,000	Fig. 13(b)
1	0.02	0.2	0.1	1.5	10,000	Fig. 13(c)
1	0.04	0.2	0.1	1.5	10,000	Fig. 13(d)
1	0.06	0.2	0.1	1.5	10,000	Fig. 13(e)

space domain is also increased and the number of labyrinth is decreased. The same for the Fig. 12(h) for $\delta = 5$, the number of the spotted area in the space domain is increased. Finally, if we increase the diffusion coefficient, system (3.5) exhibits a pattern transition from labyrinth pattern to spotted pattern.

We will choose b as a parameter of bifurcation since it determines the ratio of two factors which are the birth rates of the prey and the predator. In Fig. 13, we show the effect of the bifurcation parameter on the formation of patterns for the two species predator prey at time $t = 10,000$. All values of the used parameters are summarized in Table 3. The left column is the evolution of the prey spatial pattern and the right one is the predators. We see from these figures (Fig. 13(a) and (b)), that the labyrinth

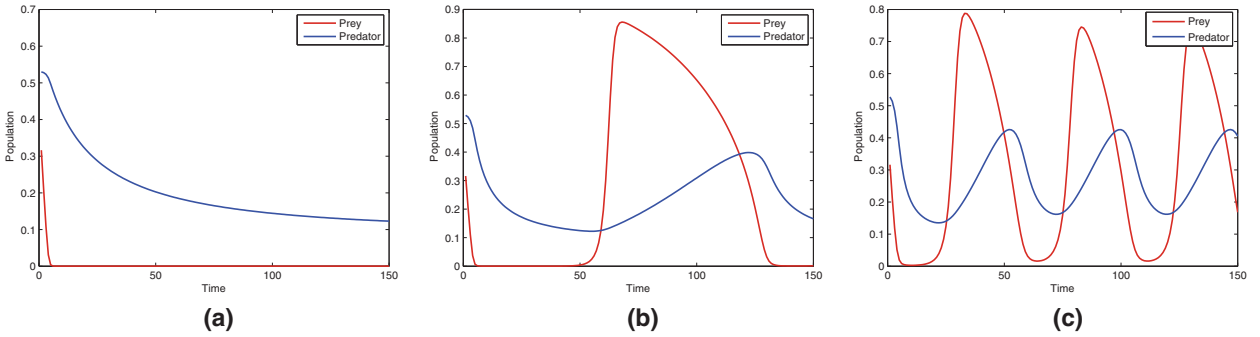

Fig. 14. Solution curves of prey-predator populations when the bifurcation parameter b varies.

Table 4
The values of parameters model, and the corresponding pictures of patterns are shown (Figs. 14 and 15).

Values of a	Values of b	Values of e_1	Values of e_2	Values of δ	Values of t	Contour pictures
1	0.001	0.2	0.1	1	150	Fig. 14(a)
1	0.04	0.2	0.1	1	150	Fig. 14(b)
1	0.075	0.2	0.1	1	150	Fig. 14(c)
1	0.001	0.2	0.1	1	550	Fig. 15(a)
1	0.0037	0.2	0.1	1	550	Fig. 15(b)
1	0.02	0.2	0.1	1	550	Fig. 15(c)
1	0.065	0.2	0.1	1	550	Fig. 15(d)

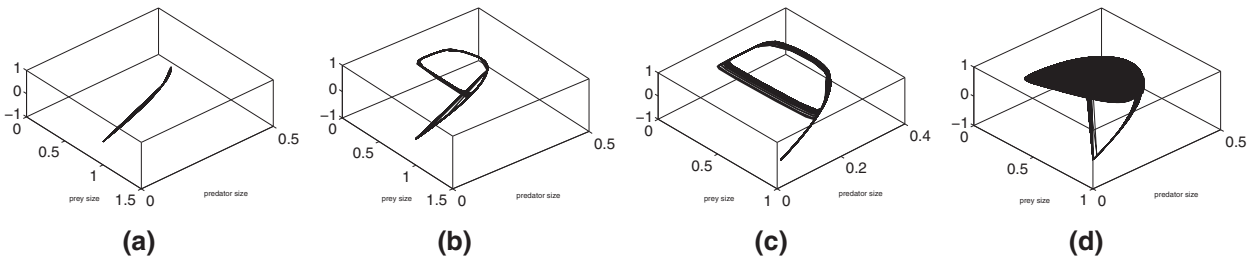

Fig. 15. Phase plane trajectories (U, V) of prey-predator populations, for system (3.5), for different values of b, $b = 0.001$ (a), $b = 0.0037$ (b), $b = 0.02$ (c), $b = 0.065$ (d).

patterns prevail in the whole domain. From Fig. 13(c), we see that the spotted and labyrinth patterns prevail in the whole domain if we increase the bifurcation parameter $b = 0.02$ and spotted pattern prevail over the whole domain at last (Fig. 13(d) and (e)) at $b = 0.04$ and $b = 0.06$.

In Fig. 14, we plot the curves of densities of prey and predator with respect to time t when the bifurcation parameter b varies. All values of the used parameters are summarized in Table 4. We observe from this Figure that populations of prey-predator converge to their steady states with the passage of time and $E^* = (u^*, v^*)$ is locally asymptotically stable for system (3.5). If we increase the value of the bifurcation parameter $b = 0.075$ the equilibrium $E^* = (u^*, v^*)$ loses its stability and becomes unstable Fig. 14(c).

For better studying the properties of the population dynamics as a whole, we estimate the species size of prey and predator by

$$U(t) = \int_0^R \int_0^{2\pi} u(t, r, \theta) dr d\theta \qquad \text{and} \qquad V(t) = \int_0^R \int_0^{2\pi} v(t, r, \theta) dr d\theta. \tag{6.12}$$

In what follows, we will study the properties of the oscillations of the dynamics of the populations when one varies the bifurcation parameter. Therefore, while b varies between 0.001 and 0.065 and the other parameters are fixed as in Table 4, we leave a rather large transitory time. We start with $b = 0.001$, then the equilibrium is globally stable see Fig. 15(a). If we increase the bifurcation parameter we have a bifurcation when this ratio is equals to $b = 0.0037$. When b belongs to $[0.0037, 0.02]$ the system exhibits periodic trajectory, see Fig. 15(b) and (c). Finally, the chaotic dynamic takes place Fig. 15(d). Fig. 16 shows the evolution of the spatial pattern of prey and predator at $\delta = 1.5$ at different time steps, with small random perturbation of the stationary solution u^* and v^* of the spatially homogeneous systems, other parameters are fixed as in Table 5. One can see from this figure that the labyrinth patterns prevail over the whole domain and this labyrinth is almost stable over time.

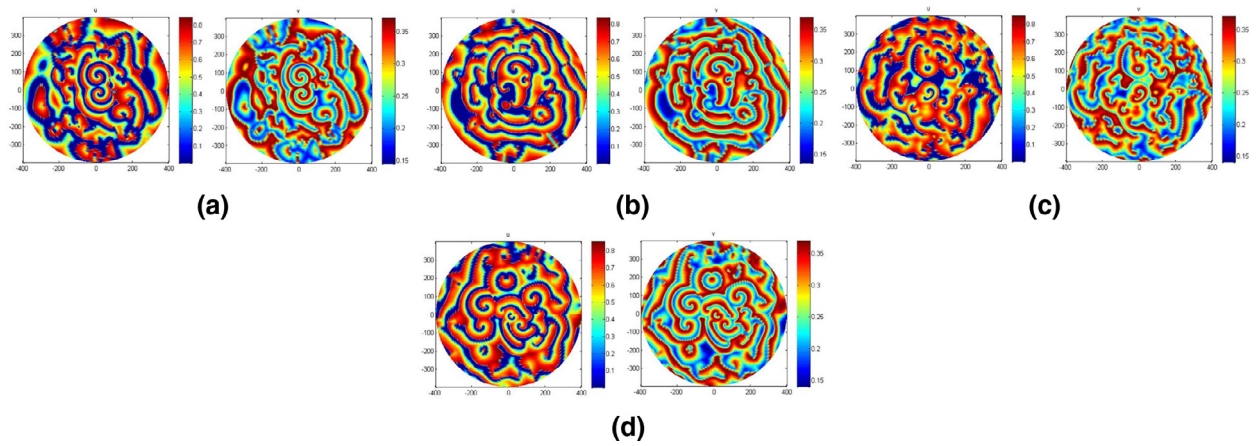

Fig. 16. Spatial distribution for fixed δ, b and time varying.

Table 5
The values of parameters model, and the corresponding pictures of patterns are shown (Fig. 16).

Values of a	Values of b	Values of e_1	Values of e_2	Values of δ	Values of t	Contour pictures
1	0.01	0.2	0.1	1.5	8000	Fig. 16(a)
1	0.01	0.2	0.1	1.5	10,000	Fig. 16(b)
1	0.01	0.2	0.1	1.5	12,000	Fig. 16(c)
1	0.01	0.2	0.1	1.5	15,000	Fig. 16(d)

7. Conclusion

In this paper, we present the analysis of two developed predator-prey systems in the last decades in ecology. For this, we have presented a spatio-temporal prey-predator system given by a reaction–diffusion equations which is based on a Holling-type *II* modified functional responses. We assumed that the two populations diffuse in a disc domain $\{(x, y) \in \mathbb{R}^2 / x^2 + y^2 < R^2\}$. Initially, we presented the model on the circular domain (i.e. polar coordinate $\mathcal{D} = \{(r, \theta) : 0 < r < R,\ 0 \leq \theta < 2\pi\}$ and analyzing the nature of the eigenvalues of the Laplacian on a circular domain. The local and global stabilities of the interior steady state are studied as well as bifurcations which lead to the instability of this equilibrium.

The numerical simulations indicate that the effect of the diffusion coefficient and the bifurcation parameter for pattern formation is remarkable. From the patterns exhibited through Figs.–9 one can see that the stripe patterns prevail over the whole domain at last and the dynamics of the system does not undergo any further changes.

We found that if we increase the diffusion coefficient, system (3.5) exhibits a pattern transition from labyrinth pattern to spotted pattern (Fig. 12). Therefore, one can predict that the effect of diffusion coefficient can be considered as an important mechanism for the appearance of complex spatio temporal patterns in spatial predator prey model.

Our aim in the next paper is to show the theoretically the results observed via numerical simulations such spatio-temporal chaos, patterns induced by Turing instability and Hopf instability of the system (3.5).

Acknowledgement

We are very grateful to the Editor and to the anonymous Referees for their valuables remarks and suggestions which help us to improve the quality of the present paper.

References

[1] M.A. Aziz-Alaoui, Study of a Leslie-Gower-type tritrophic population model, Chaos Soliton Fract. 14 (8) (2002) 1275–1293.
[2] M.A. Aziz-Alaoui, M. Daher Okiye, Boundedness and global stability for a predator-prey model with modified Leslie-Gower and holling type II shemes, Appl. Math. Lett. 16 (2003) 1069–1075.
[3] E. Beretta, Y. Kuang, Global analyses in some delayed ratio-depended predator–prey systems, Nonlinear Anal. Theor. Meth. Appl. 32 (3) (1998) 381–408.
[4] B.I. Camara, M.A. Aziz-Alaoui, Dynamics of predator-prey model with diffusion, Dyn. Cont. Discret. Impul. Syst. A 15 (2008) 897–906.
[5] A.F. Nindjin, M.A. Aziz-Alaoui, M. Cadivel, Analysis of a predator-prey model with modified Leslie-Gower and Holling-type II schemes with time delay, Nonlinear Anal. Real World Appl. 7 (5) (2006) 1104–1118.
[6] B.I. Camara, M.A. Aziz-Alaoui, Turing and Hopf patterns formation in a predator prey model with Leslie-Gower type functional response, Dyn. Cont. Discret. Impul. Syst. B 16 (2008) 897–906.
[7] S.B. Hsu, Constructing Lyapunov functions for mathematical models in population biology, Taiwan. J. Math. 9 (2) (2005) 151–173.
[8] A.F. Nindjin, M.A. Aziz-Alaoui, Persistence and global stability in a delayed Leslie-Gower type three species food chain, J. Math. Anal. Appl. 340 (1) (2008) 340–357.
[9] B.I. Camara, Complexité de dynamiques de modèles proie-prédateur avec diffusion et applications (Ph.D. thesis), Le Havre University, France, 2009.

[10] M. Daher Okiye, M.A. Aziz-Alaoui, On the dynamics of a predator-prey model with the Holling-Tanner functional response, in: V. Capasso (Ed.), Proceedings of the ESMTB Conference, MIRIAM Editions, 2002, pp. 270–278.
[11] C. Letellier, M.A. Aziz-Alaoui, Analysis of the dynamics of a realistic ecological model, Chaos Solut. Fract. 13 (1) (2002) 95–107.
[12] C. Letellier, L. Aguirre, J. Maquet, M.A. Aziz-Alaoui, Should all the species of a food chain be counted to investigate the global dynamics, Chaos Sol. Fract. 13 (5) (2002) 1099–1113.
[13] B. Fiedler, A. Scheel, Spatio-Temporal Dynamics of Reaction-Diffusion Patterns, Trends in Nonlinear Analysis, in: M. Kirkilionis, S. Krömker, R. Rannacher, F. Tomi (Eds.), Springer-Verlag, Berlin, 2003.
[14] X. Liu, Y. Loub, Global dynamics of a predator–prey model, J. Math. Anal. Appl. 371 (2010) 323–340.
[15] R. Xu, M.A.J. Chaplain, Persistence and global stability in a delayed predator-prey system with Michaelis–Menten type functional response, Appl. Math. Comput. 130 (2002) 441–455.
[16] L. Hei, Global bifurcation of co-existence states for a predator–prey–mutualist model with diffusion, Nonlinear Anal. Real World Appl. 8 (2) (2007) 619–635.
[17] M. Daher Okiye, Study and asymptotic analysis of some nonLinear dynamical systems: Application to predator-prey problems (Ph.D. thesis), Le Havre University, France, 2004 (in French).
[18] J. Huang, G. Lu, S. Ruan, Existence of traveling wave solutions in a diffuse predator prey model, J. Math. Biol. 46 (2003) 132–152.
[19] J.D. Murray, Mathematical Biology: II. Spatial Models and Biomedical Applications, Springer-Verlag, Berlin Heidelberg, 2003.
[20] F. Yi, J. Wei, J. Shi, Bifurcation and spatiotemporal patterns in a homogeneous diffusive predator-prey system, J. Differ. Equat. 246 (2009) 1944–1977.
[21] M. Baurmanna, T. Grossb, U. Feudela, Instabilities in spatially extended predator-prey systems: Spatio-temporal patterns in the neighborhood of Turing-Hopf bifurcations, J. Theor. Biol. 245 (2007) 220–229.
[22] R. Yafia, F. El Adnani, H. Talibi, Limit cycle and numerical similations for small and large delays in a predator-prey model with modified Leslie-Gower and Holling-type II scheme, Nonlinear Anal. Real World Appl. 9 (2008) 2055–2067.
[23] R. Yafia, F. El Adnani, H. Talibi, Stability of limit cycle in a predator-prey model with modified Leslie-Gower and Holling-type II schemes with time delay, Appl. Math. Sci. 1 (3) (2007) 119–131.
[24] R. Yafia, M.A. Aziz Alaoui, Existence of periodic travelling waves solutions in predator prey model with diffusion, Appl. Math. Model. 37 (6) (2013) 3635–3644.
[25] Garvie, Finite-Difference Schemes for Reaction Diffusion Equations Modeling Predator Prey Interactions in MATLAB Mathematical Biology, School of Computational Science, Florida State University, Tallahassee, FL, USA, 2013, pp. 32306–4120.
[26] L.N. Guin, P.K. Mandal, Spatiotemporal dynamics of reaction–diffusion models of interacting populations, Appl. Math. Model. 38 (2014) 4417–4427.
[27] L.N. Guin, P.K. Mandal, Spatial pattern in a diffusive predator-prey model with sigmoid ratio-dependent functional response, Int. J. Biomath. 07 (2014) 1450047, doi:10.1142/S1793524514500478.